The Pennsylvania State University

The Graduate School

Department of Materials Science and Engineering

BIAS ELECTRIC FIELD DEPENDENCE OF HIGH POWER CHARACTERSTICS IN PZT PIEZOELECTRIC CERAMICS

A Thesis in

Materials Science and Engineering

by

Anushka Bansal

Submitted in Partial Fulfillment
of the Requirements
for the Degree of

Master of Science

August 2017

The thesis of Anushka Bansal was reviewed and approved* by the following:

Kenji Uchino
Professor of Electrical Engineering
Thesis Advisor

Joan Redwing
Professor of Materials Science and Engineering,
Chemical Engineering and Electrical Engineering
Associate Director, Materials Research Institute

Qiming Zhang
Distinguished Professor of Electrical Engineering

Suzanne E. Mohney
Professor of Materials Science and Engineering
Chair, Intercollege Materials Science and Engineering Graduate Degree Program

*Signatures are on file in the Graduate School

ABSTRACT

Lead Zirconate Titanates (PZT's) have been overwhelmingly concentrated on and have commanded the most recent 60 years in piezoelectric applications. Even though material constants for piezoelectric ceramics are for the most part described under free conditions, these measured properties are not legitimate specifically when devices work under externally applied high mechanical or electrical loads. The properties of these materials are liable to the conditions in which they are measured. In this way, an essential point of examination right now is the behavior of these ceramics under such external conditions. DC bias stress and electric field are of specific significance for study because the actuators and transducers are frequently utilized as a part of these conditions to balance out or improve the operation performance. Apart from working under externally applied loads, piezoelectric materials are utilized as a part of diverse high power applications, for example, ultrasonic motors and submerged sonar transducers. In these devices, the piezoelectric materials are driven under high voltages and currents. At high power conditions, the materials go astray from their linear constitutive conditions because of non-linearity and hysteresis in physical parameters. The hysteresis manifests in terms of loss and consequently, heat generation in piezoelectric materials. In this way, the properties must be measured in practically-identical high power testing situations to accomplish significant estimations. Thus, investigation of the loss mechanisms is essential in the determination of heat generation.

This thesis means to illuminate the loss mechanisms in piezoelectric ceramics in the perspective of the late advancements in high power piezoelectric devices affected by externally applied DC bias field. Under a high mechanical excitation condition at the resonance of a piezoelectric specimen, measured by edge vibration velocity (RMS), the mechanical quality factor

Q_m degraded by 22% per 0.1 m/s of the vibration velocity increment for the soft PZT, while 17% per 0.1 m/s for the hard PZT under a DC bias field of 300 V/mm. However, it increased by 3.1% per 100 V/mm for the soft and 1.7% per 100 V/mm for the hard PZT with the applied positive DC bias field under a constant vibration velocity of 0.3 m/s. The high-power properties deviated significantly from the ones measured under low power conditions (15% increase in elastic compliance whereas Q_m degraded by a factor of 2 under a DC bias field of 100 V/mm). Therefore, this study concludes that the deterioration of the mechanical quality factor Q_m with an increase in vibration velocity can be recovered by externally applying positive DC bias field. The DC bias field 200 V/mm exhibits an almost equivalent “opposite” change rate to the vibration velocity of 100 mm/sec.

Also, to investigate the loss mechanisms, the three losses (dielectric, elastic and piezoelectric losses) were determined under low and high power conditions. Mechanical loss tan ϕ’ displayed a change of 2.5% per 100V/mm for soft PZT and 1.1% per 100V/mm for the hard PZT, whereas the dielectric loss showed a change of nearly 1.5% per 100V/mm for soft PZT and 0.4% per 100V/mm for hard PZT. It is notable that the piezoelectric loss tan θ’ can be decreased most effectively under the positive DC bias field (3.1% per 100 V/mm for the soft PZT and 1.9% per 100 V/mm for the hard PZT), than the elastic or dielectric losses. Another noteworthy point is the two-step mechanism observed in hard PZT, a bend of the slope is observed in the elastic loss tan ϕ’ on the vibration velocity change, while a bend of the slope in the dielectric constant is observed on the DC bias field change. This may suggest a sort of threshold value in terms of mechanical stress or electrical field for stabilizing/unstabilizing the domain wall motions.

TABLE OF CONTENTS

LIST OF FIGURES

LIST OF TABLES

ACKNOWLEDGEMENTS

First, I would like to express sincere gratitude to my advisor, Dr. Kenji Uchino for giving me the opportunity to work with him throughout my graduate years. It was an honor to be under his personal and academic guidance. He provided me the courage and enthusiasm for conducting research. He has been very supportive towards my research and has provided valuable comments when I got stuck. He also encouraged me to engage in collaborative research. I would also like to thank Office of Naval Research for supporting this study with their funding through Dr. Kenji Uchino.

I would like to extend my appreciation to my master's thesis committee members: Prof. Joan Redwing and Prof. Qiming Zhang for taking their time and contributing to my thesis. Their valuable comments and suggestions lead to various new approaches and made my thesis broader from the fundamental materials science viewpoint.

I would also like to thank to my past ICAT colleague Dr. Husain Shekhani for providing additional aspects to my research. Also, Maryam Majzoubi and Minkyu Choi for being there, not just as coworkers, but also as friends when I needed them. My thesis would not be possible without the collaboration in the past years with Mr. Eberhard Hennig and Dr. Timo Scholehwar from PI ceramics. I would like to extend my thanks to them for not only providing me samples but many scientific discussions that helped me throughout.

Last but not the least, I would also like to thank all my family members and friends. My family, especially my parents, Mukund and Manju Bansal and my brother Yashasvi Bansal gave me their support when I needed them the most. Feeling the warmth of my family helped me to keep my courage when I was down. My friends at Penn State made the graduate life more fun and less stressful.

OUTLINE

The first chapter reviews the fundamentals of the piezoelectricity and gives examples of piezoelectric materials. Initially, piezoelectric materials will be explained in chronological order. Then, piezoelectric materials will be grouped into three depending on the structure. Also, origin of losses in piezoelectric ceramics (i.e. mechanical, dielectric, and piezoelectric) through hysteresis will be outlined later in the section. After this, importance of measuring high power properties and external constraints in piezoelectric materials will be explained.

The second chapter gives a summary of different electrical characterization techniques. In the first part, mechanical quality factor at resonance and antiresonance will be introduced. In the latter half, different techniques that could be used to completely characterize the ceramics will be explained. Complete characterization of the piezoelectric ceramic includes calculating the mechanical quality factor, electromechanical coupling factor, both "real" and "imaginary" parts of dielectric permittivity, elastic compliance and piezoelectric constant. The electrical characterization in this thesis have been performed under two power level: low power (0.5-1 V_{rms}/mm) and high power (>1V_{rms}/mm) conditions. Low power characterization using Continuous Admittance Spectrum method will then be described later. At the end, high power characterization using Burst mode will be explained.

The third chapter explains the motivation and objectives of the work performed. It briefly reviews the path of thinking involved in carrying out the current research work. It explains the conditions under which material properties were measured earlier and the critical need to measure the material coefficients under externally applied mechanical and electrical constraints.

Next, in the fourth chapter, the experimental method for continuous admittance spectrum analysis for low power measurements have been described. Also, experimental method for Burst mode technique to measure high power properties have been described. In this section, the focus is on obtaining measurements of low and high power measurements on piezoelectric materials in k_{31} vibration modes.

Based on the experimental techniques developed, the results for low power performance and high power performance piezoelectric ceramics are summarized in chapter 5.

The last chapter is a synopsis of the results explained in the dissertation. The summary will also include conclusions followed by a broad range of recommended future work in chapter.

Chapter 1
Background

1.1 Piezoelectricity:

The disclosure of the capacity of crystals, for example, Quartz, Topaz and Rochelle Salt, among others, to generate electric charge when subjected to mechanical stress is ascribed to the Curie brothers who observed this interest at some point in 1880[1]. This phenomenon was immediately named piezoelectricity, to discern it from at the time already established thoughts of friction based electricity and pyroelectricity. The converse phenomenon, however, was not discovered but rather thermodynamically predicted one year later, and after that immediately demonstrated experimentally. [2]

A dielectric material (dielectric for short) is an electrical insulator that can be polarized by an applied electric field. In such dielectrics, when an electric field is applied, electrical charges are attracted to different directions, due to the nature of electrostatic interactions. In lieu of this movement, electric dipoles are generated all throughout the material. This phenomenon is known as electric polarization. . In ionic dielectric materials, the constituent atoms are charged (ionized) in a certain orientation and magnitude. These materials can store charge due to the electric charge per unit area called dielectric displacement D and dielectric polarization P.[3] It can be represented by the given equation:

$$D = \varepsilon_0 E + P = \varepsilon \varepsilon_0 E \qquad (1.1.1)$$

where ε_0 is the permittivity in vacuum (ε_0=8.854 x 10^{-12} F/m) and ε is the material's relative permittivity.

There are seven crystal systems based on the degree of symmetry: triclinic, monoclinic, orthorhombic, tetragonal, trigonal (rhombohedral), hexagonal and cubic. These basic crystal systems are classified into 32 point groups per the crystallographic symmetry. [4] Out of these, 21 are non-centrosymmetric (no inversion center). Among those 21 point groups, except group 432, crystals having all other point groups exhibit “piezoelectric” effect. [5] 10 out of 20 non- centrosymmetric point groups have a spontaneous polarization. These polar point groups that have a finite polarization possess both piezoelectric and pyroelectric effects. Temperature dependence of the spontaneous polarization in the crystal creates ‘pyroelectricity’. For such crystals, temperature change creates an electric charge on the surface of the crystals as a result of the change in the spontaneous polarization. These materials show natural spontaneous polarization (P_s) in the structure without the application of an electric field. Materials possess spontaneous polarization below a specific temperature, which is the Curie temperature (T_c). If the spontaneous polarization of a pyroelectric material can be reversed, then the material is called, ferroelectric. [6] Relationship between these materials exists as shown in Fig. 1.1.1.

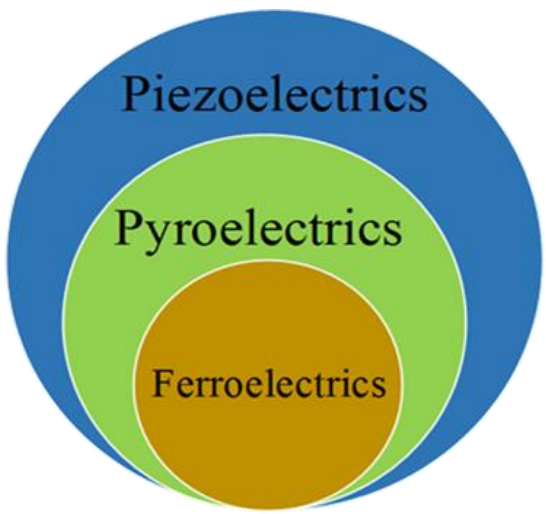

Figure 1.1.1 Relationship between materials that possess piezoelectricity, pyroelectricity and ferroelectricity.

Piezoelectricity is a coupling phenomenon between electrical energy and mechanical energy which emerges from the non-centrosymmetric unit cell. These materials develop surface charges in response to an applied pressure (direct piezoelectric effect), and create mechanical strain in response to an applied electric field (converse piezoelectric effect), which can then be used for sensing and actuating purpose respectively. [7] The direct as well as converse piezoelectric effects can be visualized in Fig. 1.1.2.

The direct and converse phenomenon can be represented by the following constitutive equations containing stress X, strain x, electric field E and dielectric displacement D:

$$x_i = s^E_{ij} X_j + d_{mi} E_m \qquad (1.1.2)$$

$$D_m = d_{mi} X_i + \varepsilon^X_{mk} E_k \qquad (1.1.3)$$

where, i, j=1, 2,…,6; m,k=1,2,3 represent the tensor subscripts. Here, s^E, d and ε^X are the compliance at constant electric field, the piezoelectric constant and permittivity at constant elastic stress respectively. [6]

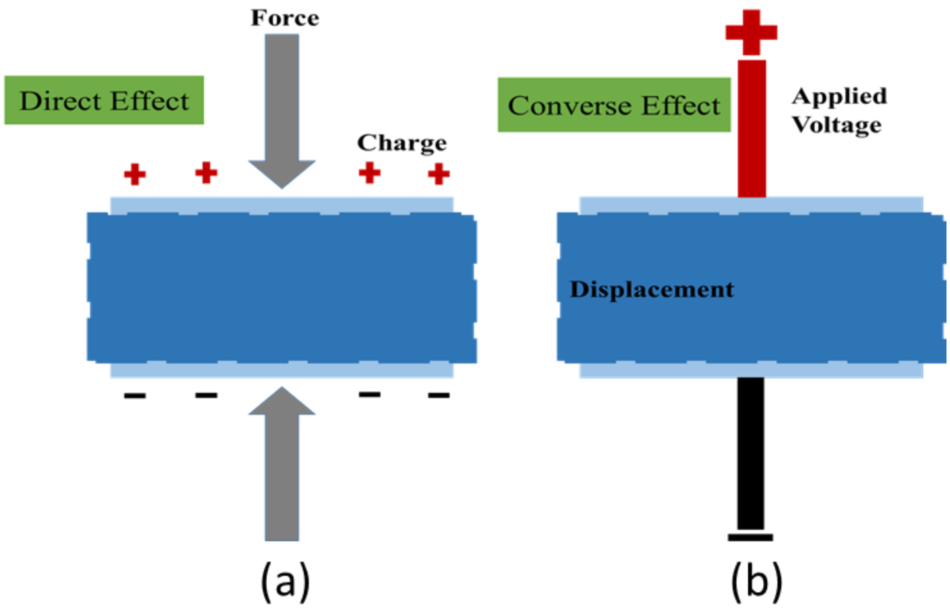

Figure 1.1.2 (a) Direct piezoelectric effect and (b) converse piezoelectric effect

1.2 Properties of Piezoelectric Ceramics:

1.2.1 Hysteresis and Losses

Piezoelectric materials, for example, Lead-Zirconate Titanates [$Pb(Zr_xTi_{1-x})O_3$, PZT's] have widely been adopted for many applications such as underwater sonars, motors, and piezoelectric

transformers. [8] To scale down the piezoelectric actuators and transducers, high power-density piezoelectric material developments are required for realizing the same level of mechanical vibration energy in a smaller specimen, without temperature ascend through internallosses. [9] The efficiency and reliability of piezoelectric materials are directly related with their hysteresis or loss characteristics. The hysteresis is a critical issue in precise positioning under off- resonance working conditions for piezoelectric applications. Particularly, in resonance applications, loss or hysteresis generates noteworthy amount of heat in the piezoelectric material because of the heat accumulation in a short period. There are three types of losses; mechanical loss, dielectric loss and piezoelectric loss. [10] Ikeda clarified the basic loss mechanisms in piezoelectric ceramics by dismissing the piezoelectric loss. Loss mechanisms were further clarified by introduction of complex physical parameters. Late research by Uchino and Hirose made an exhaustive explanation of the loss mechanisms and calculation of the loss parameters in piezoelectric ceramics. [11], [12] Each loss component is categorized into intensive and extensive groups. Per IUPAC (The International Union of Pure, and Applied Chemistry), extensive parameter depends on the volume of the material, while intensive parameter is the ratio of two extensive ones, and therefore, is independent on the volume of the material. Consequently, stress (X) and electric field (E) are intensive parameters, which are externally controllable; while strain (x) and dielectric displacement (D) (or polarization (P)) are extensive parameters, which are internally determined in the material. The “intensive” or “extensive” dielectric, elastic, piezoelectric losses are defined asa time lag measured under X, E constant (or free), or under x, D (or P) constant conditions, respectively. Formulations with time delay (phase lag) can be represented as follows:

$$\varepsilon^{X*} = \varepsilon^{X}(1 - j\tan\delta'), \quad (1.2.1) \qquad \beta^{x*} = \beta^{x}(1 + j\tan\delta), \quad (1.2.4)$$

$$s^{E*} = s^{E}(1 - j\tan\phi'), \quad (1.2.2) \qquad c^{D*} = c^{D}(1 + j\tan\phi), \quad (1.2.5)$$

$$d^{*} = d(1 - j\tan\theta'), \quad (1.2.3) \qquad h^{*} = h(1 + j\tan\theta). \quad (1.2.6)$$

Here, j is the imaginary notation, ε^X is the dielectric constant under constant stress, β^x is the inverse dielectric constant under constant strain, s^E is the elastic compliance under constant electric

field, c^D is the elastic stiffness under constant electric displacement, d is the piezoelectric constant, and h is the inverse piezoelectric charge constant. Note that the tensor components of β is not just an inverse value of ε, but an inverse tensor component of the ε matrix in a 3D model. The extensive losses appear in a constraint condition such as mechanically-clamped or electrically-open circuit, and are often used to discuss the physical materials performance. The intensive (prime) tangents should have the negative sign, while the extensive (non-prime) tangents take the positive sign, so that both tangents can keep the positive sign as experimentally determined values in general. The loss tangent value should be much smaller than 1 (less than 0.1 in practice) in this complex parameter usage, and means a phase/time lag of the output parameter (such as P) from the input parameter (such as E). The phase lags, which were explained above, can be observed experimentally (Fig. 1.2.1). It shows experimentally observed hysteresis curves for strain (x) – stress (X) (short-circuit condition), dielectric displacement (D) – electric field (E) (stress-free condition), strain (x) – electric field (E) (stress-free condition) and dielectric displacement (D) – stress (X) (open-circuit condition). These phase lags are defined as intensive losses. Note that the hysteresis areas on x – E or D – X domains are not directly related with the piezoelectric loss, but with coupled loss with elastic or dielectric losses, as indicated on the figures.

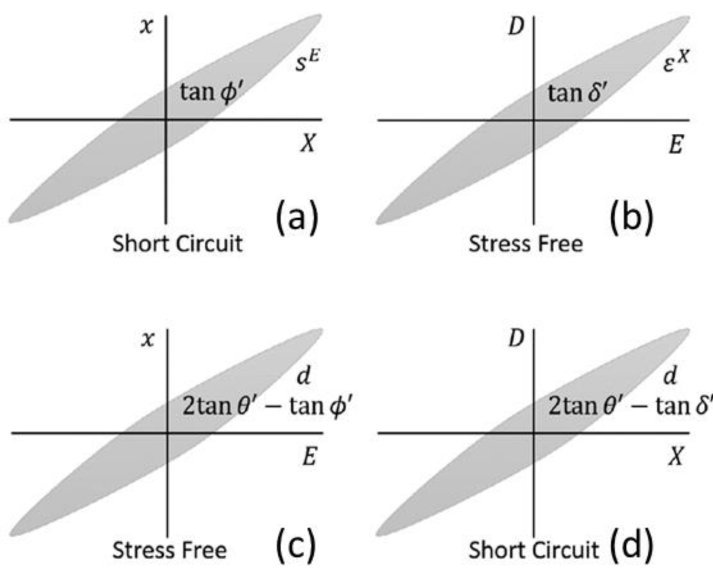

Figure 1.2.1 (a) x-X (short circuit), (b) D-E (stress-free), (c) x-E (stress-free) and (d) D-X (open circuit)

When there is no phase lag (δ=0), all stored electric energy is recovered after a full cycle with 100% efficiency. Since the hysteresis corresponds to loss, the area inside the hysteresis loop, Fig. 1.2.1 (a) corresponds to the energy loss per cycle per unit volume and can be represented as (1.2.7). The lost energy is dissipated as heat in the dielectric material. This is also why tan δ' is named as the dissipation factor. The stored electric energy, U_e can be represented by (1.2.8). One can apply the same concept to the stored and loss mechanical energy (Fig. 1.2.1(b)) and represent as (1.2.9) and (1.2.10), respectively.

$$w_e = \pi \varepsilon^X \varepsilon_0 E_0^2 tan\delta' \qquad (1.2.7)$$

$$U_e = \frac{1}{2}\varepsilon^X \varepsilon_0 E_0^2 \qquad (1.2.8)$$

$$U_m = \frac{1}{2} s^E X_0^2 \qquad (1.2.9)$$

$$w_m = \pi s^E X_0^2 tan\Phi' \qquad (1.2.10)$$

The electromechanical stored (U_{em} and U_{me}) and loss energy (w_{em} and w_{me}) under an applied electric field and stress respectively can be represented as follows:

$$U_{em} = \frac{1}{2}\frac{d^2}{s^E} E_0^2 \qquad (1.2.11)$$

$$w_{em} = \pi \frac{d^2}{s^E} E_0^2 (2tan\theta' - tan\,\phi') \qquad (1.2.12)$$

$$U_{me} = \frac{1}{2}\frac{d^2}{\varepsilon^X \varepsilon_0} X_0^2 \qquad (1.2.13)$$

$$w_{me} = \pi \frac{d^2}{\varepsilon^X \varepsilon_0} X_0^2 (2tan\theta' - tan\delta') \qquad (1.2.14)$$

Therefore, to advance the power level of piezoelectric devices it is necessary to clarify the loss phenomenology and mechanism. Note that the intensive and extensive losses are interrelated by a so-called K-matrix of the coupling factor, given by

$$\begin{bmatrix} \tan\delta' \\ \tan\phi' \\ \tan\theta' \end{bmatrix} = [K] \begin{bmatrix} \tan\delta \\ \tan\phi \\ \tan\theta \end{bmatrix} \qquad (1.2.15)$$

$$[K] = \frac{1}{1-k^2}\begin{bmatrix} 1 & k^2 & -2k^2 \\ k^2 & 1 & -2k^2 \\ 1 & 1 & -1-k^2 \end{bmatrix},\ k^2 = \frac{d^2}{s^E(\varepsilon^T \varepsilon_0)} = \frac{h^2}{c^D(\beta^S/\varepsilon_0)} \qquad (1.2.16)$$

Intensive loss components of the three can be obtained from the resonance and anti-resonance mechanical quality factors in the k_{31} mode, while the extensive loss components can be obtained from the mechanical quality factors in the k_{33} mode. In this thesis, to make the situation simplest, we will be focusing on the intensive losses. However, extensive losses can be determined indirectly using the K matrix.

Mechanical quality factors also play a significant role in the loss study of piezoelectrics. They are basically related to dielectric, elastic and piezoelectric loss factors. Besides, a higher quality factor at the antiresonance is usually observed in the PZT based piezoelectric materials, in comparison with the resonance quality factor. However, the previous theory without considering the piezoelectric loss factor could not explain the deviation of the resonance quality factor Q_A and antiresonance quality factor Q_B explicitly. IEEE Std. only provided the method to derive Q_A based on the equivalent circuit, and assumed that the resonance quality factor is equal to the antiresonance quality factor from a traditional thought. Quality factor (Q) compares the time constant for decay of a resonating system's amplitude to its resonance period. It is generally defined as:

$$Q = 2\pi \frac{Energy\ Stored}{average\ energy\ dissipated\ per\ cycle} \qquad (1.2.17)$$

1.3 Losses under High Power Conditions

The drive to miniaturize components and the search for higher efficiency in battery operated devices are driving the development of piezoelectric components to replace less efficient electromagnetic analogs. [13], [14] All these new piezoelectric devices are operated at resonance, since on off-resonance ceramics requires high electric voltage/electric field for a certain magnitude of strain (0.1%). Benefitting from amplification of the strain that occurs at the resonance under a reasonably

small electric field to obtain the highest vibration amplitudes/velocities for a similar level of strain (0.1%). In this condition, excited vibration amplitudes are substantially high and significant heat is generated through losses, which limit the usable vibration amplitude level of the piezoelectric. A simple rule of thumb-figure-of-merit is the maximum vibration velocity. This can be viewed as a figure to evaluate the maximum mechanical energy density generated in a piezoelectric ceramic material, while limiting the temperature rise in the piezoelectric 20^{o}C higher than room temperature. [13] - [17] Note that the practical upper-limit of vibration velocity is restricted by heat generation, since above a certain vibration level increasing hysteretic effects (increasing losses) result in thermal instability. Though the off-resonance driven piezoelectrics generate heat in a rather homogeneous matter in a specimen, the resonance-driven piezoelectrics generate heat in an inhomogeneous manner. The temperature profile follows the strain distribution and the heat is concentrated at the nodal points. Temperature difference of 20 degrees from room temperature is observed typically within a 10 % of the sample size in the piezoelectric (fig. 1.3.1). Thus, significant attention must be paid to the generated heat (losses), as it might result in premature failure of the actuator.

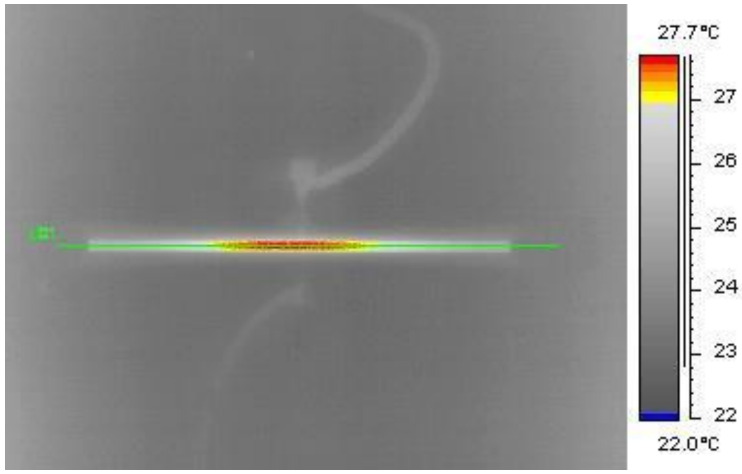

Figure 1.3.1 Heat generation in a piezoelectric ceramic at resonance conditions

1.4 Losses under External DC Bias Field

Material constants for piezoelectric ceramics are for the most part described under free conditions, but these measured properties are not valid specifically when devices work under externally applied high mechanical or electrical loads. The properties of these materials are liable to the conditions in which they are operated. DC bias stress and electric field are of specific significance for study because the actuators and transducers are frequently utilized as a part of these conditions to balance out or improve the operation performance.

There has been a lot of early work on the dependence of material constants of piezoelectric ceramics on external DC bias field under low power conditions. [20], [21] In early 1970s and 1980s, researchers studied extensively on the dependence of dielectric constant as a function of externally applied DC bias field. They concluded that when the electric field is applied, the dielectric constant changes depending on the degree of domain motion or the value of applied DC bias field. In 2000, G. Yang et. al studied the effects DC Bias Field on the Piezoelectric, Dielectric, and Elastic Properties of Piezoelectric Ceramics. [22] Most of the observations of the results obtained by them were based on the extrinsic contributions to the piezoelectric response that arises from the existence of domains in the ceramic materials. They showed that the piezoelectric d33 constant shows a slight decrease when a positive DC bias is applied on the specimen. Over the entire range of negative DC bias that was applied, the value of d33 for the hard PZT increased significantly and no drop in the value of d33 was observed. In the case of soft PZT, they found that significant depoling started even at the low bias field of - 0.5 MV/m. They concluded that, in applications where a large driving field must be applied to piezoelectric materials, the field dependent non-linearity plays an important role. For soft materials, the occurrence of depoling should be considered if the material is likely to be subjected to a negative field. Also in 2003, similar work was performed by A. J Masys et. al. They studied the strain levels in ferroelectric ceramics as a function of electric field and determined the piezoelectric coefficients d_{33}, d_{31}, and d_{15} of different types of PZT ceramics as a function of electric field. [21] They concluded that in general, for both hard and soft PZT, the piezoelectric coefficient showed significant nonlinearity with increasing field strength. Higher d coefficients were realized with the application of a negative dc bias. However, depoling and repoling occurred in soft PZT under high bias fields. Positive bias fields resulted in a slight decrease in the d coefficients due to domain wall pinning. Also, in 2003, Q. M Wang et. al directly studied the effect of DC bias field on the complex piezoelectric, dielectric and elastic coefficients of a piezoelectric ceramic resonator under various DC bias field. [23] It has been found that with DC bias increasing, elastic compliance, piezoelectric coefficient and dielectric permittivity decrease with approximately linear relationships. Since the resonance frequency of the piezoelectric resonator changes with the applied DC bias field, it is suggested that the DC bias field can be used for frequency tuning or frequency–temperature stability control in device applications. Various results obtained by the researchers over the years have been plotted in fig 1.4.1.

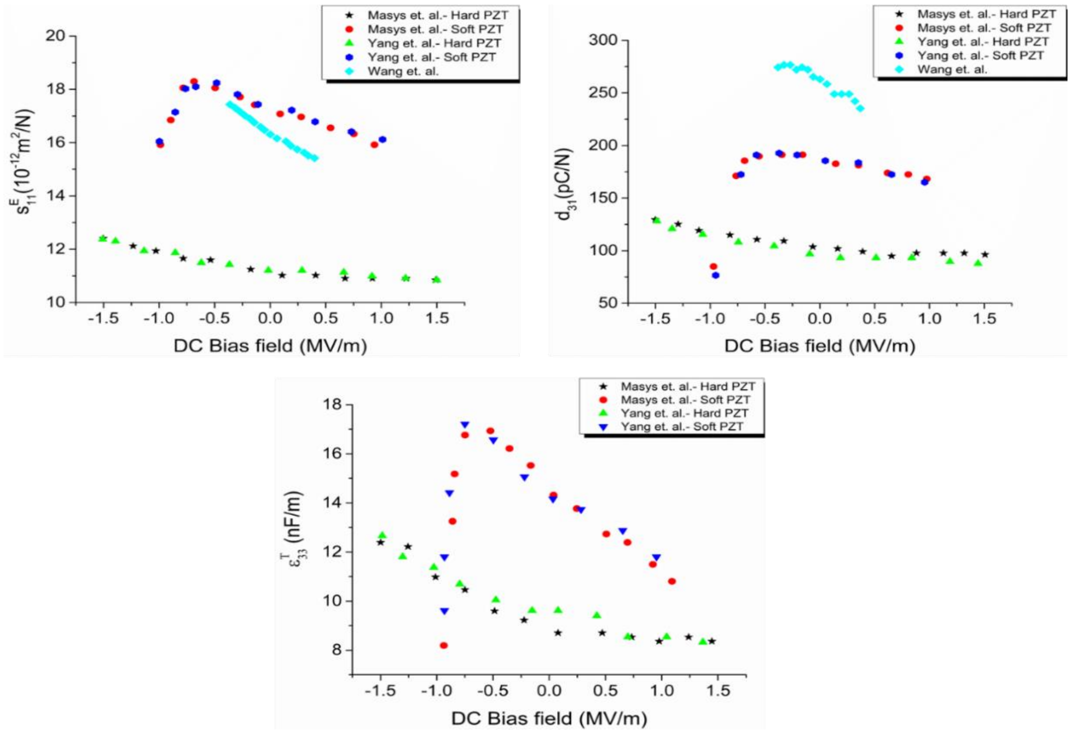

Figure 1.4.1 Various results obtained by researchers to obtain the dielectric constant, elastic constant and piezoelectric constant as a function of DC bias field over the years.

Although much work has been performed in order the evaluate the material constants for the piezoelectric constants at low power, little work has been performed to measure the losses under different external conditions. Thus, it becomes need of the hour to evaluate the loss behavior for the piezoelectric ceramics at low and as well as high power conditions.

Chapter 2
Characterization Methods

In piezoelectric studies, materials characterization is trailed by both electrical and mechanical characterization. Piezoelectric materials, for example, PZT, Lead Titanate ($PbTiO_3$), have been broadly utilized as sensors, actuators, transducers also, resonators for some electromechanical applications. Properties of piezoelectric materials are essential parameters in materials determination for device outline and manufacture. For the most part, a total characterization of piezoelectric materials incorporates the assurance of piezoelectric coefficients, dielectric permittivity, elastic coefficients, mechanical quality factor, and electromechanical coupling coefficients. These properties are generally measured by the methods suggested by the IEEE norms. However, it has been brought up that the IEEE standard strategy is not appropriate to characterize loss behavior in piezoelectric materials. Precise characterization ought to treat all the previously mentioned materials coefficients as complex numbers so that the loss component can be measured. Generally, economically accessible analyzers or meters e.g. impedance analyzers, d_{33} and LCR meters are utilized to measure low power properties. However, they cannot be used to measure high power performance of the device. The ICAT group at The Penn State University has been working extensively to characterize the ceramics under high power conditions by developing special characterization methodology, HiPoCS (High Power Piezoelectric Characterization System). ICAT designed system have been used to carry out experiments for this work. This chaptergives an overview of the methods used for characterizing the ceramic at both low as well as high power conditions.

2.1 Piezoelectric Resonance & Antiresonance

Presently, characterization of piezoelectric ceramics includes fundamentally working at resonance, antiresonance and off resonance conditions. Before hopping on to the formulae for computing real and imaginary parts of the elastic, piezoelectric and dielectric complex, it turns out to be essential to comprehend the importance of the diverse conditions under which measurements are performed.

The resonance state of a piezoelectric oscillator is characterized as the condition where a oscillating input voltage instigates a greatest current response. The antiresonance state of a piezoelectric component is characterized as the condition in which a swaying input current results in a most extreme voltage response. When an electric field is applied to the piezoelectric ceramic, along the polarization direction, then as per the Poisson's ratio, the material expands in one direction and contracts in the perpendicular direction. Accordingly, this example can display methods of vibration along the thickness, length, and width. Resonance and Antiresonance are either mechanical resonance or electromechanical coupling resonance modes. The mechanical resonance frequency is related just with the sound speed in the material and the geometry. The thickness extensional mode (k_{33} mode) experiences mechanical resonance at the electrical antiresonance frequency comparing to the consistent D condition, while the length extensional mode (k_{31} mode) experiences mechanical resonance at the electrical resonance frequency because of the steady E, which then changes the sound speed in the material. The extensional type resonators of k_{31}; k_{33}; and k_p are the most widely recognized extensional vibration modes utilized for piezoelectric devices. The geometries for each of these resonators is given in Fig. 2.1.1. However, only k_{31} is examined in this work.

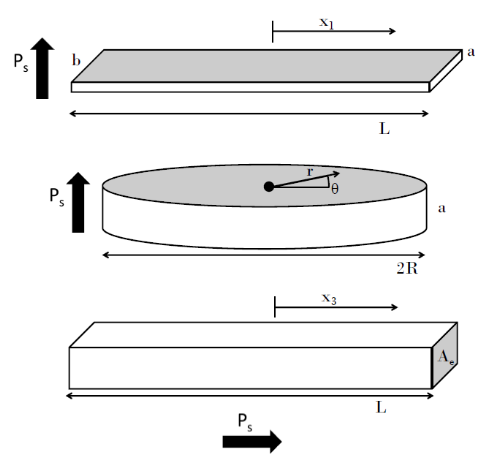

Figure 2.1.1 Various geometries for piezoelectric ceramics

2.2 Low Power Characterization

Low power properties were measured using continuous admittance spectrum method. Now, one may think of a thought of only a basic characterization like low power characterization used in commercially available analyzers with constant input voltage method. This is not perfect since when we deal with a constant voltage, the piezoelectric materials tend to give large nonlinear elastic behavior ju st around the resonance area. The issue is that amid the frequency sweep, there is a jump phenomenon on voltage and current around the resonance. This jump phenomenon is because of the expanded elastic non-linearity of piezoelectric material as the driving level (e.g. current) increments This issue can be overcome by making estimations under consistent vibration velocity instead of constant voltage with an enhanced equal circuit by embracing the proportionate constants for every vibration level. This method also revealed the anti-resonance region in the frequency spectra.

The properties were calculated from the continuous admittance spectrum sweeping from slightly below resonance frequency to slightly above the antiresonance frequency by keeping the vibration velocity (i.e., constant stored mechanical energy). [30]

Mechanical quality factor at the resonance as well as antiresonance (Q_A and Q_B respectively) for the k_{31} mode (fig. 3.2.1) was calculated based on the frequency difference between two frequencies corresponding to the 3 dB below the admittance resonance peak and the impedance anti-resonance peak. Taking narrow frequency range close to the resonance (fig. 2.2.2) and anti-resonance, we can define the resonance quality factor (Q_A) and the anti-resonance quality factor (Q_B) as shown in equation (3.2.1). In this research, the difference between two quality factors, Q_A and Q_B calculated at resonance and antiresonance respectively was investigated.

$$Q_{A,31} = \frac{f_A}{f_1 - f_2} \text{ and } Q_{B,31} = \frac{f_B}{f_1 - f_2} \qquad (2.2.1)$$

where f_A and f_B are the resonance and antiresonance frequencies respecively; f_1- f_2 is the 3dB bandwidth.

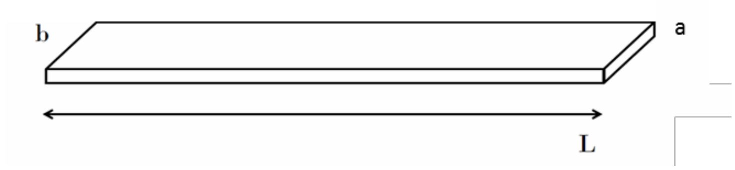

Figure 2.2.1 A rectangular PZT plate with all the dimensions marked (L: length, b: width, a: thickness).

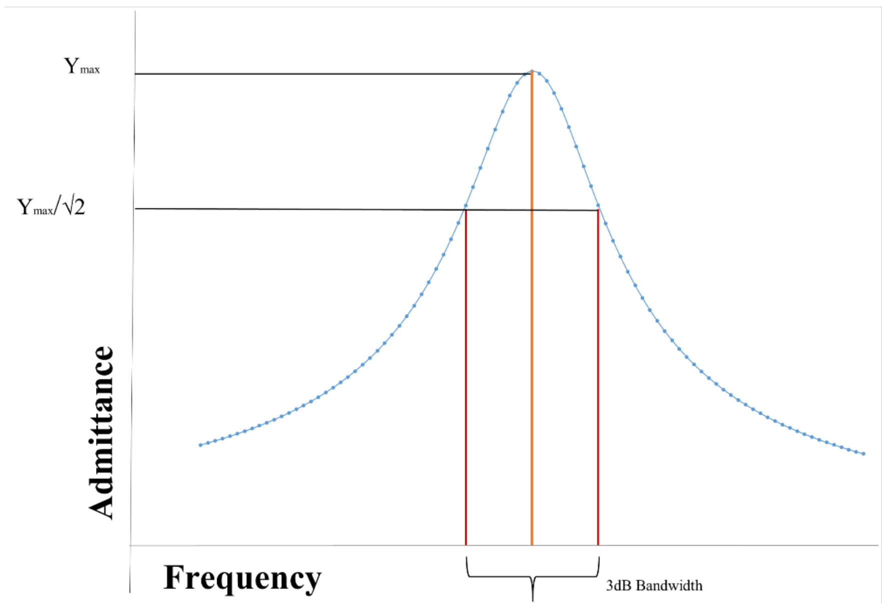

Figure 2.2.2 3 dB bandwidth method to calculate Q_A at the resonance frequency

Intensive loss components of these three can be obtained from the resonance and anti- resonance mechanical quality factors Q_A and Q_B in the k_{31} mode from the following equations:

$$Q_{A,31} = \frac{1}{\tan \phi_{11}'} \tag{2.2.2}$$

$$\frac{1}{Q_{B,31}} = \frac{1}{Q_{A,31}} + \frac{2}{1 + (\frac{1}{k_{31}} - k_{31})^2 \Omega_{B,31}{}^2} (\tan \delta_{33}' + \tan \phi_{11}' - 2 \tan \theta_{31}') \tag{2.2.3}$$

Here k_{31} is the electromechanical coupling factor, $\tan\delta_{33}'$, $\tan\phi_{11}'$, $\tan\theta_{31}'$ are loss factors for ε_{33}^{T}, s_{11}^{E}, d_{31}, respectively. The parameter $\Omega_{B,31}$ is proportional to the anti-resonance frequency ω_b:

$$\Omega_{B,31} = \frac{\omega_b l}{2v_{11}^{E}} \tag{2.2.4}$$

where v_{11}^{E} is the sound velocity of the material in the direction of length L, ρ is the density and is given by $v_{11}^{E} = 1/\sqrt{(\rho s_{11}^{E})}$.

The elastic compliance s_{11}^{E} can be calculated from the resonance frequency as

$$s_{11}^{E} = 1/((2Lf_A)^2\rho \tag{2.2.5}$$

The electromechanical coupling factor k_{31} is defined by:

$$k_{31}{}^2 = \frac{d_{31}{}^2}{s_{11}^{E}(\varepsilon_{33}{}^{X}\varepsilon_0)} \tag{2.2.6}$$

where d_{31} is the piezoelectric constant, s_{11}^{E} is the elastic compliance at a constant electric field, ε_{33}^{T} is the free (unclamped) permittivity, ε_0 is the permittivity in vacuum. Electromechanical coupling factor k_{31} can be calculated from the resonance and antiresonance frequencies as

$$k_{31}^2 = \frac{\frac{\Pi f_B}{2 f_A}.\tan(\frac{\Pi}{2}\frac{f_B - f_A}{f_A})}{1+\frac{\Pi f_B}{2 f_A}.\tan(\frac{\Pi}{2}\frac{f_B - f_A}{f_A})} \tag{2.2.7}$$

Now, to obtain tan ϕ’, Q_A is measured and inverse value gives elastic loss. Then, knowing tan δ’ from the LCR meter at the off-resonance frequency, evaluating Q_B, we can calculate tan θ’ using Eq. 2.2.3.

2.3 High Power Characterization

Dielectric and electromechanical properties of piezoelectric materials are typically reported under low electric signal conditions. This is due to the ease of measurements with standard characterization instruments (e.g. impedance analyzers and LCR meters). These instruments are usually capable of making measurements between 0.5 V_{rms}/mm and 1 V_{rms} /mm. This type of characterization is called *low power electrical characterization* due to its low excitation conditions. However, in reality, piezoelectric devices face higher driving conditions (high power) at their service conditions. Particularly, piezoelectric materials driven under resonance dissipate more and undistributed heat compared to the ones driven under off-resonance. Furthermore, when high driving conditions meet with resonance drive, substantial amount of heat is generated on the nodal point in the materials due to the increased losses. Materials' properties change when they are driven under high power levels. For example when the material is under high driving levels (e.g. vibration level (v)), hysteresis loss tends to increase and the mechanical quality factor (Q_m) degrades accompanied by the temperature increase (ΔT). The temperature increase is proportional to the driving level and above a certain level, temperature starts to increase in proportion to the power. These relations lead the vibration amplitude to be the main figure of merit when high power materials are studied. The less affected (less Q_m degradation, less ΔT increase) by the higher vibration amplitudes the material is, the better the high-power performance will be. Consequently, solely the low power characterization is not sufficient to examine the piezoelectric materials' properties because we cannot observe the change in the piezoelectric properties as in the real working conditions. Subsequently, a characterization technique should be developed to analyze the high power performance of the piezoelectric ceramic. [24], [25]

Now, the HiPoCS characterization system is capable of doing high power measurements by two methods:

1) Continuous Admittance Spectrum Method.
2) Burst/ Transient Mode.

Out of these two methods of characterization, Burst/ Transient Mode is used in this thesis because of the following reasons:

Table 1 Table comparing two methods of characterization

Continuous Admittance Spectrum Analysis	Burst/ Transient Mode
Long measurement times	Very short measurement times
Temperature rise	No temperature rise
Higher complexity of control	Simple Analysis

Spectrum analysis is primary electrical excitation method, while the burst mode is mechanical excitation method. Since we would like to eliminate the temperature rise effect in our scientific analysis viewpoint, we adopted primarily the burst mode for high power characterization. However, from the industrial/practical application viewpoint, there is some criticism on the burst mode, because this method does not include practical temperature rise in the performance evaluation.

In the Burst Mode, the ceramic is initially electrically driven at its resonance (or antiresonance) frequency for a small number of cycles (typically around 10 – 100 cycles) to excite the mechanical vibration. [25] Because of the short period excitation (less than 1 ms), practical temperature rise does not occur in the sample (less than 0.02°C) even under a high vibration excitation. Then, either a short or open circuit condition is imposed after removing or isolating the excitation electric power. In this case, when the sample oscillates at the resonance frequency and the short-circuit condition is imposed, rendered current is proportional to the vibration velocity (i.e., the ratio provides Force Factor A). Whereas, when an open-circuit condition is imposed, generated voltage is proportional to the vibration displacement (the ratio provides Voltage Factor B), and the oscillation frequency is the antiresonance frequency. By measuring the rate of signal decay, the quality factor at the resonance or antiresonance can be calculated using the formula (Eq. 2.3.1):

$$Q = \frac{2\pi f}{\frac{2\ln(\frac{v_1}{v_2})}{(t_2 - t_1)}} \qquad (2.3.1)$$

Where v_1 and v_2 are vibration velocity at two different decay time, t_1 and t_2 (typically with $t_2 - t_1 = 1$

– 3 vibration cycles). Very short measuring time (~5 sec) for obtaining full physical parameters (via LabView software) as a function of vibration velocity under the short- or open-circuit condition is an additional attractive point in the burst mode method.

We summarize here how to determine the "real" parameters, dielectric permittivity, elastic compliance and piezoelectric constant from the burst method in the case of a k_{31} plate as shown in fig. 2.2.1. Here, L is the length, b, the width and a, the height of the PZT ceramic plate. The force factor A_{31} is calculated as the ratio of the short-circuit current i_0 over the vibration velocity v_0 at the plate length edge in the resonance, and is given by Eq. (2.3.2).

$$A_{31} = \frac{i_0}{v_0} = -2b\frac{d_{31}}{s_{11}^E} \qquad (2.3.2)$$

While, the voltage factor B_{31} is the relationship between the open-circuit voltage and displacement at the plate length edge at the antiresonance, expressed by Eq. 2.3.3).

$$B_{31} = \frac{V_0}{u_0} = \frac{2a}{L}\frac{d_{31}}{s_{11}^E \varepsilon_0 \varepsilon_{33}^x} \quad . \qquad (2.3.3)$$

It is important to note that we can obtain longitudinally-clamped permittivity $\varepsilon_{33}^x \varepsilon_0$ (effective damped permittivity) at the resonance-antiresonance frequency range (not at the off-resonance) from the ratio of the force factor A_{31} over the voltage factor B_{31} in the following formula (Eq. 2.3.4):

$$\varepsilon_0 \varepsilon_{33}^X \left(1 - {k_{31}}^2\right) = \varepsilon_0 \varepsilon_{33}^x = \frac{A_{31}}{B_{31}}\frac{a}{Lb} \qquad (2.3.4)$$

Thus, free permittivity ε_{33}^X can be calculated from the relationship with the electromechanical coupling factor. The determination of the permittivity at the resonance frequency is another attractive point of the burst method. Note that the burst mode measurement is not associated with heat generation (temperature rise can be estimated less than 0.02°C) even under very high vibration velocity. [26]

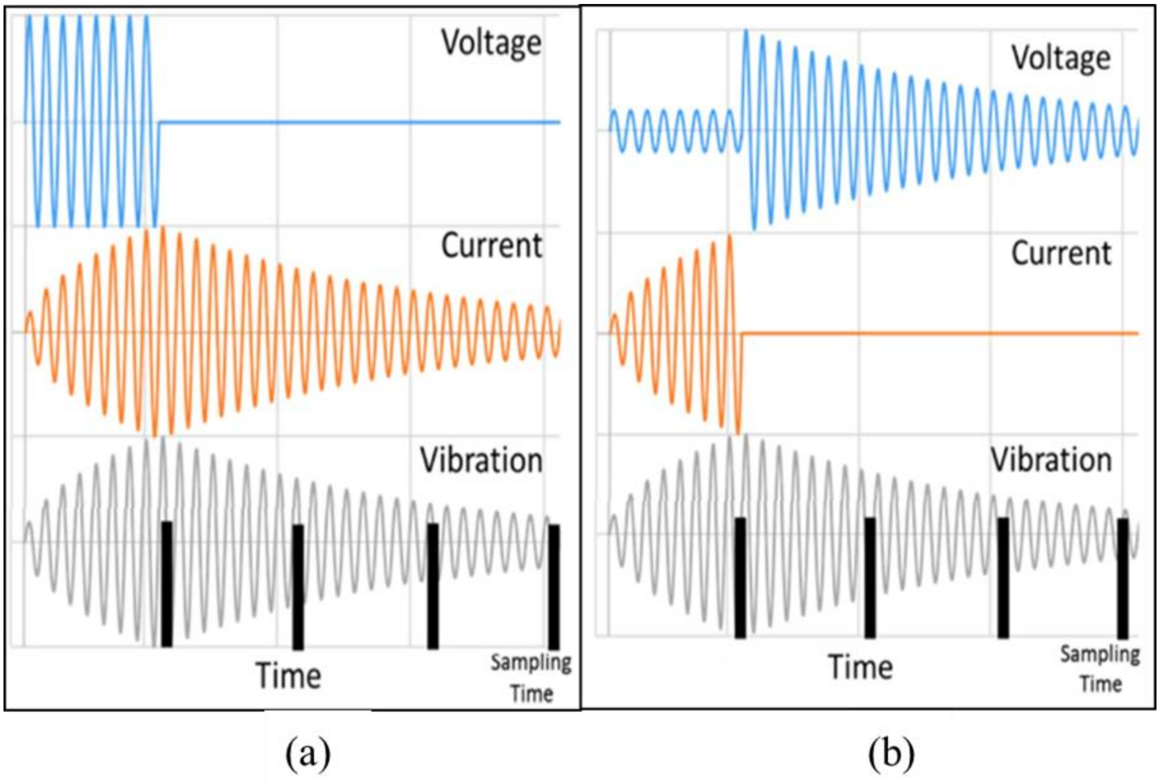

Figure 3.3.1 Conditions for Burst Mode (a) Short circuit (b) Open circuit

Chapter 3
Motivation

This thesis aims to give comprehensive understanding of loss behavior mechanisms in the piezoelectric ceramics under externally applied DC Bias field at low (0.5-1 V_{rms}/mm) as well as high power conditions (>1V_{rms}/mm). It also gives a comparative analysis between 'hard' and 'soft' PZT's and contrast the response to the externally applied electric field of the two.

Piezoelectric materials such as Lead-Zirconate Titanates [$Pb(Zr_xTi_{1-x})O_3$, PZT's] have been widely adopted for many applications such as underwater sonars, motors, and piezoelectric transformers. They have widely been contemplated and possess excellent piezoelectric properties. Modifications of PZT are widely commercialized for various applications. That is the reason PZT has commanded the piezoelectric applications since its revelation in the 1950s. A lot of research has been performed to measure losses in different modes. Yet, there has been an almost no exploration on the effect of external mechanical or external boundary conditions. Even though material constants for piezoelectric ceramics are generally depicted under free conditions, these measured properties are not valid when devices work under externally applied mechanical or electrical loads. The properties of these materials are obligated to the conditions in which they are associated. Along these lines, a basic purpose of examination right now is the lead/conduct of these ceramics under different conditions. DC Bias stress and electric field are of particular importance for study because the actuators and transducers are often used as a part of these conditions to balance out or improve the operation performance.

Regarding the bias electric field effect, previous reports clarified the stabilization mechanism of the high power performance in “Hard” $Pb(Zr,Ti)O_3$ (PZT)-based ceramics in terms of the “internal” bias field. As shown in Fig. 3.1(a), the mechanical quality factor Q_m in the hard PZT increases rather gradually after the electric poling process (~2 hours) to reach to the value higher than 1000, while the soft PZT does not change the Q_m value with time lapse. Also, the polarization versus electric field hysteresis curve change with the time lapse, where the internal “positive” electric field is created in an “aged” sample [Fig. 3.1(b)]. Accordingly, we proposed that the high Qm is primarily triggered by the “internal” bias field, which may be attributed to the defect dipoles originated from a slow rate of oxygen ion diffusion after the poling. To further explore the loss mechanism in PZT’s, instead of the “internal” bias field in hard PZT, we studied the “external” bias field effect in both hard and soft PZT’s in this thesis.

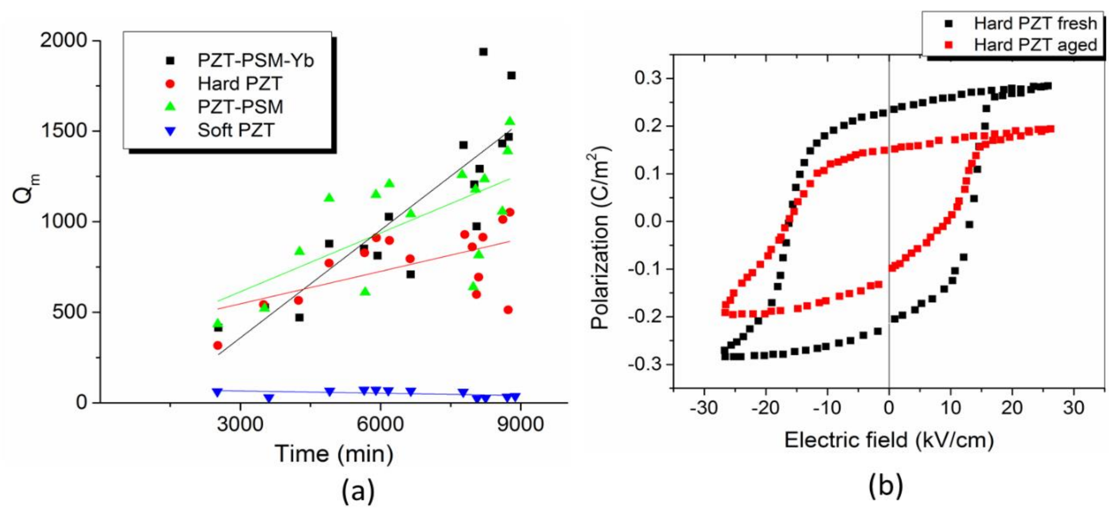

Figure 3.1 (a) Q_m as a function of time for different PZTs & P-E hysteretic response for hard PZT at different time intervals; (b) Hysteresis curve shape change with time, showing the internal bias field generation.

Likewise, piezoelectric material’s properties are typically reported at low excitation conditions (0.5-1 V_{rms}/mm). Piezoelectric ceramics behave distinctively when they are excited at high levels. High excitation conditions cause piezoelectric ceramics to build their temperature (selfheating) due to the increased losses particularly when they are driven under resonance conditions. This phenomenon becomes very critical when piezoelectric ceramics are continuously used in high power applications such as sonars, medical (e.g. therapeutic) ultrasound and piezoelectric transformers. Therefore, there is a definite requirement for understanding piezoelectric ceramics' high power characteristics to anticipate their actual performance in an application.

Different from the previous studies, this research aims at developing the loss mechanisms in piezoelectric ceramics in the k_{31} mode based on the experimental method of determining losses from the continuous admittance spectrum analysis. Moreover, this study extends over loss dependence on the form factors (k_{31} mode) in 'hard' and 'soft' piezoelectric ceramics. In addition, the study is extended to perform high power characterization apart from the low power studies. Although low power characterization techniques are favored in light of the fact that they are speedy and permit simple perception of desired electrical properties of the material. In actuality, piezoelectric devices confront higher driving conditions (high power) at their operating conditions. Materials' properties change when they are driven under high power levels. Therefore, this work will reflect the magnitude of difference in the properties and performance of the piezoelectric device under low and high power conditions.

Chapter 4
Experimental Procedures

4.1 Sample Selection

We used PIC 144 and PIC 255 as hard and soft PZT's, respectively, in this study. These PZT ceramic plates were prepared in the R&D Department, PI Ceramic GmbH (Lindenstrasse, 07589 Lederhose, Germany). All the plate samples (5pieces for each) with size of 40mm long x 5 mm wide x 0.5 mm thick were silver-electroded on 40 mm x 5 mm face. Hard PZT was electrically poled at 80^0C for 6 hours whereas soft PZT was electrically poled at 70˚C for 10 hours along the thickness in 0.5 mm.

4.2 Electrical Characterization System

High power characteristics of the PZT rectangular plates were measured by a high-power characterization system (HiPoCS), which was developed by our group (Fig. 4.2.1). An amplitude controlled sinusoidal signal was produced by a function generator (HP 33120A) and amplified (NF 4010). The sample current was detected by a clamp-on AC current sensor (Tektronix TCP 305). The voltage, current and displacement waveforms of the piezoelectric disks/transformers were monitored by two digitizing oscilloscopes (Tektronix TDS 29 3014B) and logged by a personal computer using a software interference (LabVIEW®). The temperature on the sample's nodal point was measured by an infrared spot thermometer (Hioki 3445). [28], [29] In parallel, the permittivity ε^T was measured at 1 kHz (off-resonance) by an LCR meter [SR715, Stanford Research Systems, Inc., Sunnyvale, CA]. Also, DC Bias field was applied externally using an external amplifier. Here, the bias field direction is denoted "positive" when the field is applied along the polarization direction. The range of the externally applied DC bias field varies from -160 to +320V/mm (less than 1/4 of the coercive field). Vibration amplitudes on the edge of the piezoelectric rectangular plates was measured with laser interferometer (Polytec OFV 511). The

HiPoCS is capable of measuring high power characteristics of the materials under constant current, voltage and vibration velocity modes. However, to avoid the jump phenomenon during the frequency sweep, we characterized the behavior of the mechanical quality factor under various constant vibration velocities under low power measurements using continuous impedance spectrum method.

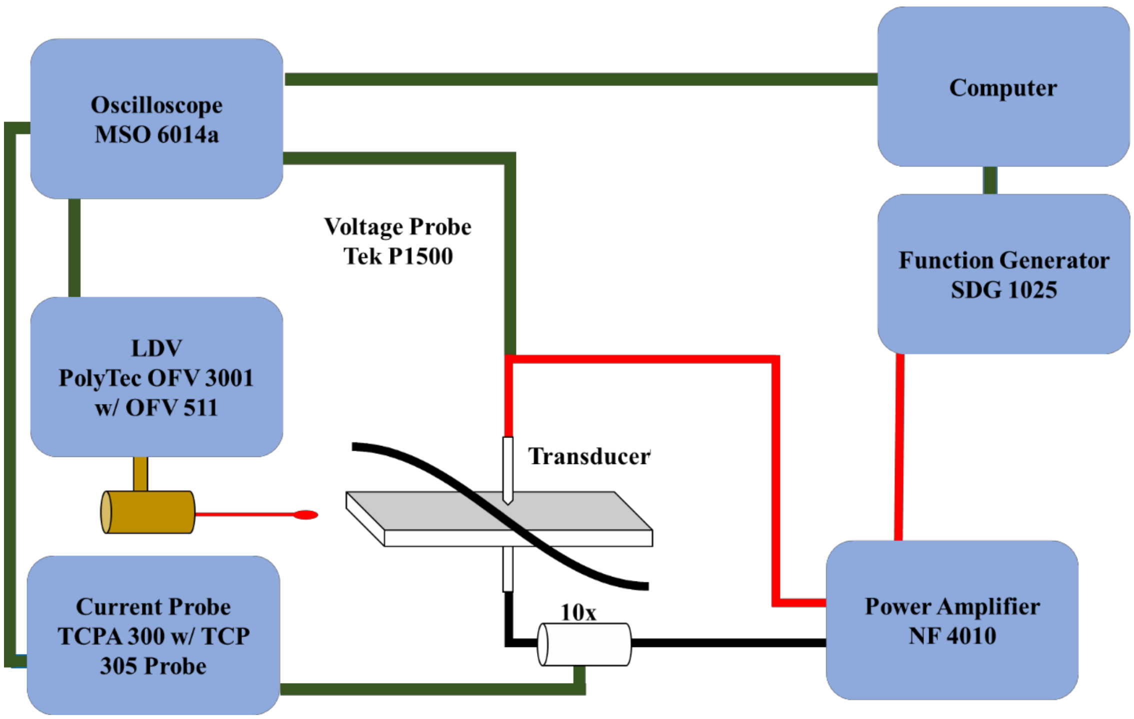

Figure 4.2.1 The High Power Characterization System (HiPoCS). [31]

Chapter 5
Experimental Results

At first, P-E loop measurements were performed for both the hard as well as soft PZT's. Figure 5.1. 1 shows the polarization versus electric field hysteresis curves at 10 Hz for hard (PIC 144) and so ft (PIC 255)PZT's (roughly 10 weeks aged). In comparison with a symmetric curve for the soft PZ T, we observed a positively biased hysteresis ($E_{bias} \approx$ 700 V/mm) curve in the hard PZT sample which verified the earlier argument about internal DC bias field already present in the hard PZT piezoelectric ceramics. The derivative of the P-E curve provides permittivity at a low frequency of 10 Hz, which is inserted in Fig. 5.2.1 and discussed later.

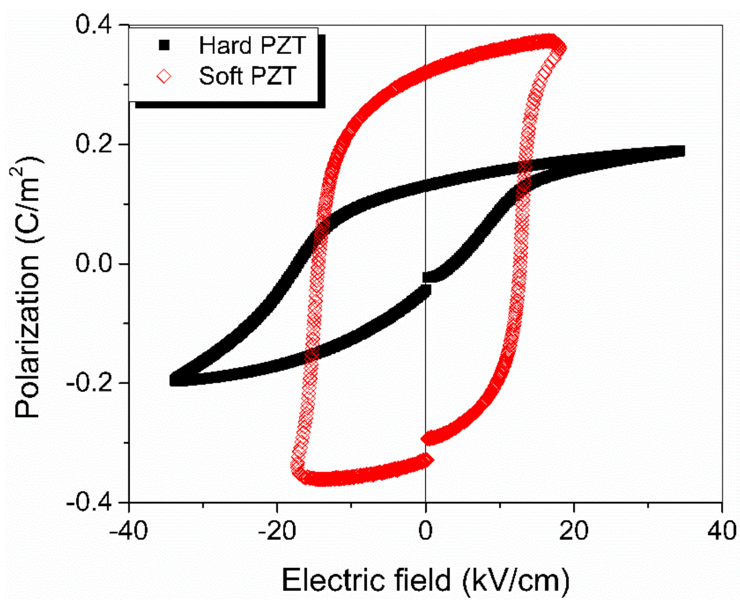

Figure 5.1 P-E hysteresis loop for hard and soft PZT's

5.1 High Power Measurements without DC Bias Field

At first, high power measurements were performed without applying external DC bias to evaluate the change of material's properties with the vibration velocity itself (no influence of external DC bias field). These measurements were performed using the Burst mode again.

5.1.1 Elastic Compliance and Elastic Loss

Figure 5.1.1 shows the elastic compliance change with the vibration velocity calculated from the resonance frequency (from Eq. (3.2.5)), measured for the hard (PIC 144) and soft (PIC 255) PZT's. Both samples exhibit a nearly linear compliance increase, where the change rate (3% per 0.1 m/s) for the hard PZT is less than the rate (5% per 0.1 m/s) for the soft PZT.

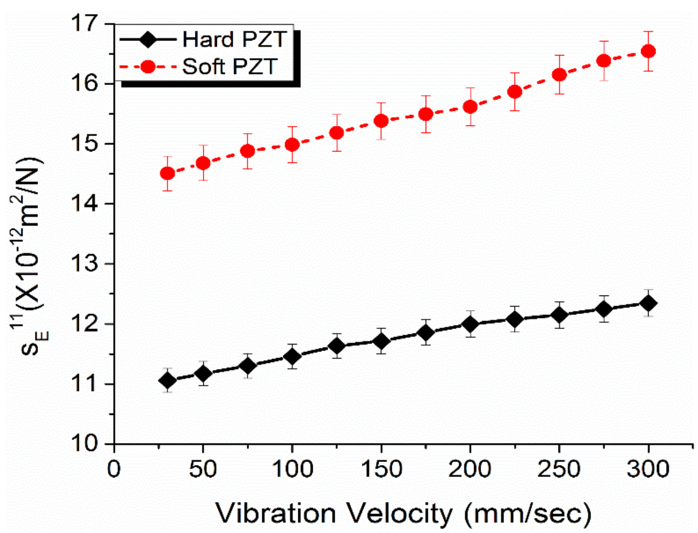

Figure 5.1.1 Elastic compliance change with vibration velocity under zero DC Bias

Figure 5.1.2(a) and 5.1.2(b) shows the quality factors at the A type resonance Q_A and at the B type resonance (i.e., antiresonance) Q_B under zero DC Bias for the hard PZT (PIC 144) and soft PZT (PIC 255) samples, respectively (Eq. (3.2.1)). Q_B is always larger than Q_A in both hard and soft PZT's, which indicates the intensive piezoelectric loss is larger than the dielectric or elastic losses in the PZT's. Taking the inverse value of Q_A, the elastic loss tan ϕ' change is plotted in Fig. 5.1.3, where the vertical axis scale differs 100 times between the hard and soft PZT's. Though both samples exhibit the elastic loss increase, the change rate of the soft PZT is rather monotonous (75% per 0.1 m/s). On the contrary, the change in the hard PZT seems to be a two-step process: almost constant up to 130 mm/s, and followed by the rate of 75% per 0.1 m/s, a similar rate to for thesoft PZT. There appears to be a threshold vibration velocity in the hard PZT, below which the sub- coercive domain wall switching may not happen significantly.

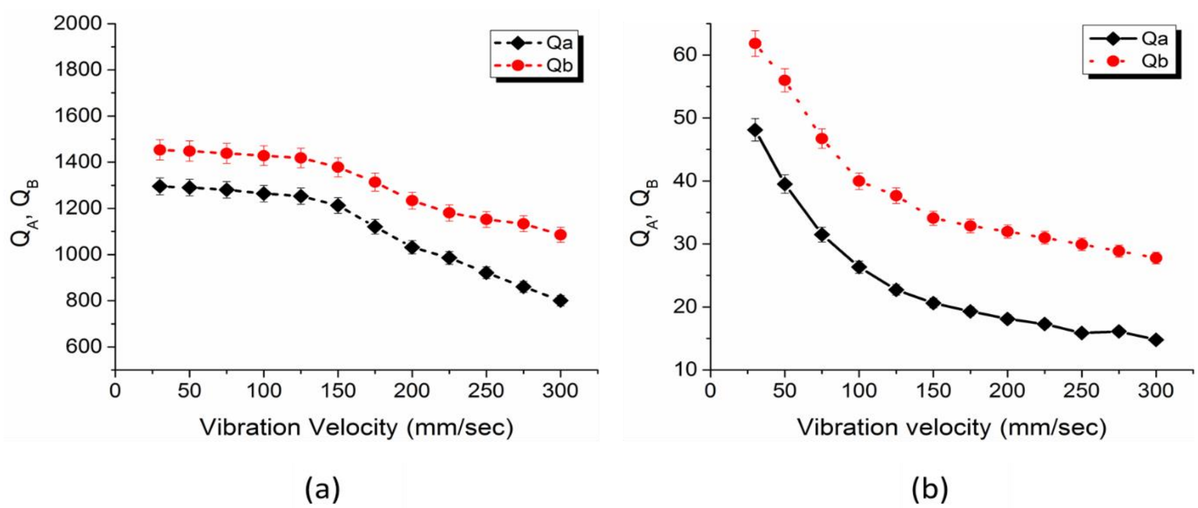

Figure5.1.2 Quality factor at A type and B type resonance for (a) PIC 144 (b) PIC 255

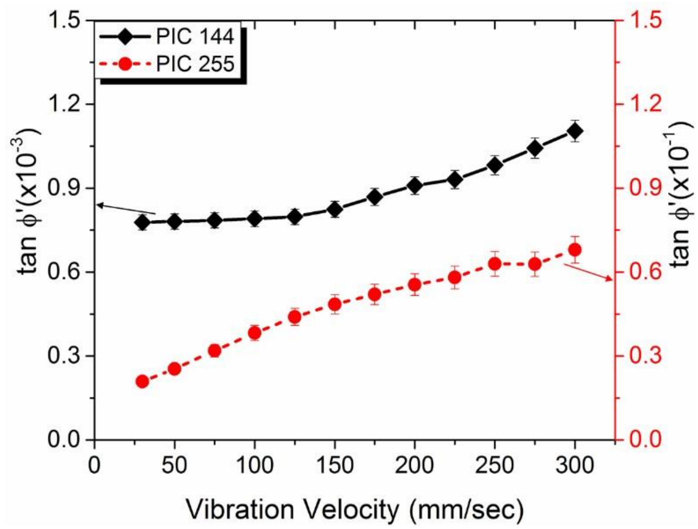

Figure 5.1.3 Elastic loss under zero DC Bias

5.1.2 Dielectric Permittivity

The dielectric permittivity at high power conditions was determined from Eqs. 3.3.3 and 3.3.4. Figure 5.1.4 shows longitudinally clamped (or effective damped) permittivity ε_{33}^{x} and free permittivity ε_{33}^{T} (calculated from the relation ε_{33}^{x}=$\varepsilon_{33}^{T}(1 - k_{31}^{2})$ with the k_{31} value obtained in the next section) as a function of vibration velocity for the both soft and hard PZT's. For comparison, ε_{33}^{T} measured at 1 kHz (off-resonance) by LCR meter is also plotted. It was observed that the calculated permittivity ε_{33}^{T} at the resonance (high frequency) is slightly lower than the one at the off-resonance 1 kHz, which is probably related to the general frequency dependence of the permittivity, supported by the ε_{33}^{T} values of 1230 (Hard) and 1610 (Soft) at 10 Hz in Fig. 5.2.1. It is noteworthy that the clamped permittivity ε_{33}^{x} also shows the increase with an increase in vibration velocity, which may be explained by the fact that this "clamp" does not mean complete clamp, but just 1D longitudinal clamp. However, since we have not established the method yet for obtaining the dielectric loss at the resonance frequency, this paper adopts tan δ' = 0.002 and 0.027 at the off-resonance (1kHz) for the hard and soft PZT's, respectively, for the loss analysis described below.

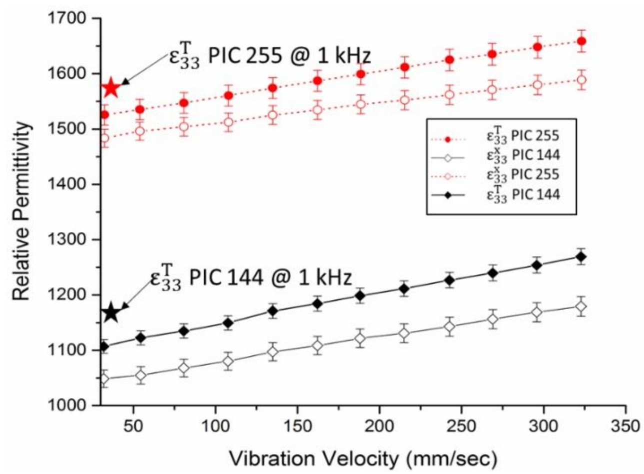

Figure 5.1.4 Relative Permittivity at zero DC Bias under high power conditions

5.1.3 Piezoelectric Constant and Piezoelectric Loss

Figure 5.1.5(a) and 5.1.5(b) shows the electromechanical coupling factor k_{31} and piezoelectric constant d_{31} change with vibration velocity for the hard and soft PZT's. The electromechanical coupling factor for both samples increased, the change rate (3.5% per 0.1 m/s) for the hard PZT is less than the rate (5.3% per 0.1 m/s) for the soft PZT. Also, the piezoelectric constant increased with increasing vibration velocity. The change rate was lower for the hard PZT (2.7% per 0.1m/s) than the soft PZT (5.1% per 0.1 m/sec).

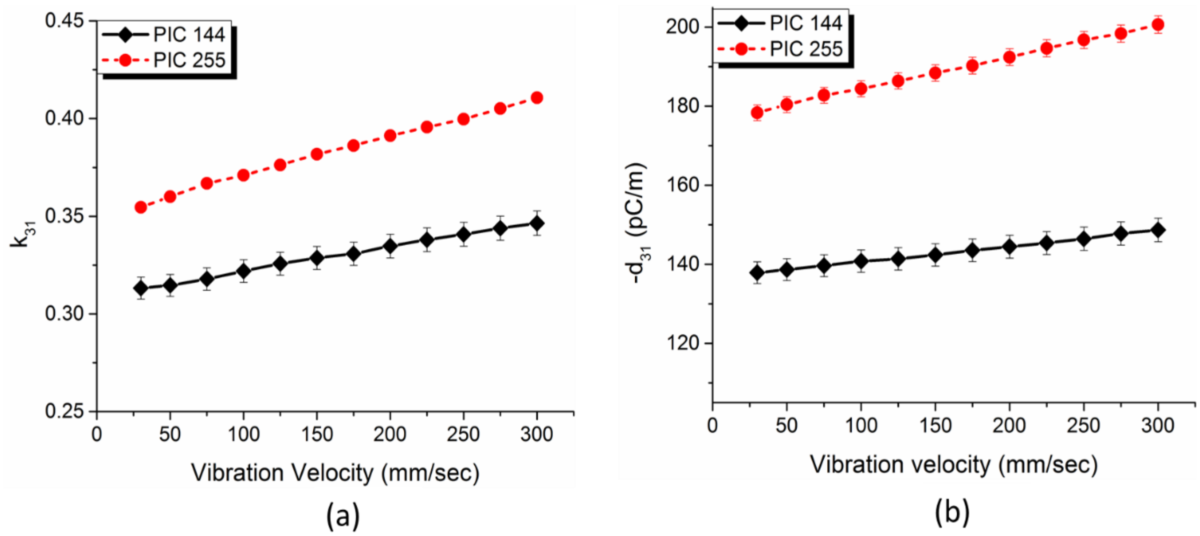

Figure 5.1.5 (a) Electromechanical coupling factor under zero DC Bias (b) Piezoelectric constant under zero DC Bias

The intensive piezoelectric loss was determined from the mechanical quality factors Q_A and plotted in Fig. 5.1.6. Note the vertical scale difference of 10 times between the hard and soft PZT's. The piezoelectric loss increases in general with vibration velocity. However, the change ratio is different. The piezoelectric loss increased by a very small factor for the hard PZT (20% per 0.1m/s) than the soft PZT (70% per 0.1m/s), which is one order of magnitude larger than the dielectric and elastic loss variation rates. It is important to note that the piezoelectric loss tan θ' increases almost linearly with vibration velocity, but there seems to be two steps in the change of mechanical loss tan φ' in the case of hard PZT: almost constant up to 130 mm/s, and followed by the rate of 75% per 0.1 m/s, similar rate to the soft PZT. This reason is under consideration from the domain dynamics viewpoint.

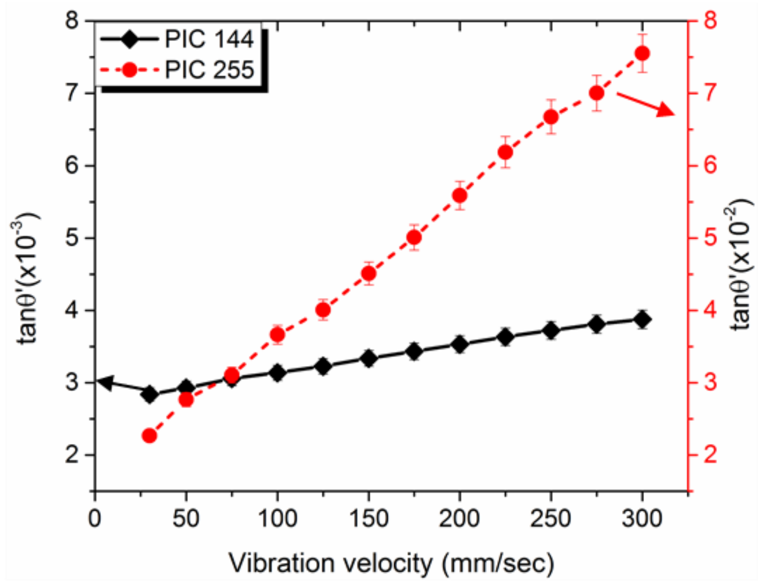

Figure 5.1.6 Piezoelectric loss under zero DC Bias

5.2 Low Power Measurements

As explained in Chapter 3 in detail, low power measurements (driving at a very small vibration velocity) were performed under externally applied DC bias field. DC bias field was varied from -160V/mm to +320V/mm using an external amplifier. The measurements were performed using Continuous Admittance spectrum method utilizing HiPoCS system. Also, the properties and the losses were calculated utilizing the formulae discussed in Chapter 3 for this specific technique.

Though the low power measurements under external DC bias field have been reported by several researchers, we performed similar experiments on the hard and soft PZT’s to perform a comparative study between low and high power measurements. Since the vibration velocity was less than 30 mm/sec, we did not observe the heat generation more than 1°C even at the resonance frequency range for both hard and soft PZT's.

5.2.1 Dielectric Permittivity & Dielectric Loss

Figure 5.2.1 (a) and 5.2.1(b) shows the dielectric permittivity and dielectric loss measured with the LCR meter at an off-resonance frequency of 1kHz (much lower than the resonance frequency ~40 kHz). As it can be seen from Fig. 5.2.1, the dielectric constant change was - 0.8% for the hard PZT and - 1.7% per 100 V/mm for the soft PZT for a positive bias field and 0.5% for hard PZT and 1.2% for soft PZT in the case of a negative bias field. Also, the dielectric constant change was - 0.8% for the hard PZT and - 1.7% per 100 V/mm for the soft PZT. As a reference, permittivity at 10 Hz as a function of DC bias field is plotted, calculated from the derivative of the P-E hysteresis curve shown in fig. 5.2.1. The dielectric permittivity at 10 Hz is larger than that at 1 kHz in both the hard and soft PZT's, which mainly caused by the different measuring methods, but a frequency dependency of the permittivity cannot be excluded at the moment. The dielectric permittivity at 10 Hz is larger than that at 1 kHz in both the hard and soft PZT's, which suggests the frequency dependency of the permittivity. In this low frequency permittivity, however, a steeper bend seems to happen around 200 V/mm and 100 V/mm for the hard and soft PZT's, which may indicate a sort of threshold of the domain wall dynamics, suggesting a two-step mechanism in terms of the DC bias field. The intensive dielectric loss tan δ' (note one order of magnitude difference between the hard and soft PZT's) shows a decreasing tendency with DC bias field with a similar bend around 200 V/mm. Though both samples did not exhibit significant dielectric loss decrease, the change rate (- 0.4% per 100 V/mm) of the hard PZT is less than the rate (- 1.5% per 100 V/mm) of the soft PZT.

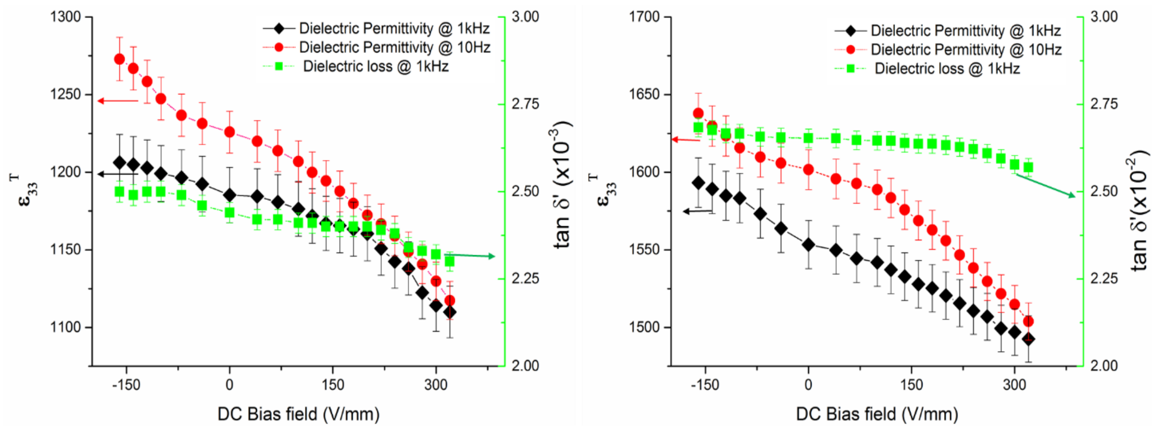

(a) (b)

Figure 5.2.1 Dielectric permittivity and the corresponding loss at 1kHz frequency for (a) Hard PZT (b) Soft PZT.

5.2.2 Elastic Compliance and Elastic Loss

Admittance spectrum method was adopted for measuring low power properties under an external electric field. High power admittance spectrum under an external field is still under consideration, because of the serious heat generation around the resonance/antiresonance region, which restricts the accurate Q_m determination. Figure 5.2.2 shows A type resonance and B type resonance (i.e., antiresonance) frequency changes with the DC bias field. Both frequencies increase monotonously with the DC field. Note that the frequency difference $\Delta f = f_B - f_A$ does not change significantly, which results in almost constant value of electromechanical coupling factor k_{31} (the change within the error bar in Fig. 5.2.3). The increase in the resonance frequency by around 1.5% for both the hard and soft PZT's was observed with increasing DC bias field, which leads to the dependence of the elastic compliance in Fig. 5.2.4 for the hard (a) and the soft PZT's (b). The % change in elastic compliance was - 0.7% per 100 V/mm for the hard PZT, in comparison to - 1.7% for the soft PZT for positive bias field and 0.5% for hard PZT and 1.4% for soft PZT in the case of negative bias field. The elastic compliance decrease with the positive DC bias field indicates that the PZT ceramics gets hardened as the DC Bias field is applied whereas effect of negative DC bias field is completely opposite.

Figure 5.2.5 represents the quality factor change with the applied DC Bias field. The quality factor at resonance Q_A (inverse of the intensive elastic loss) also increases with the applied DC bias field. The elastic loss (inverse of the mechanical quality factor) showed a shift of - 1.1% per 100 V/mm for the hard PZT and - 2.4% for soft PZT with increasing DC Bias field. Also, it showed a shift of 0.8% per 100V/mm for the hard PZT and 1.9% for the soft PZT under negative DC bias field as inserted in Fig. 5.1.4.

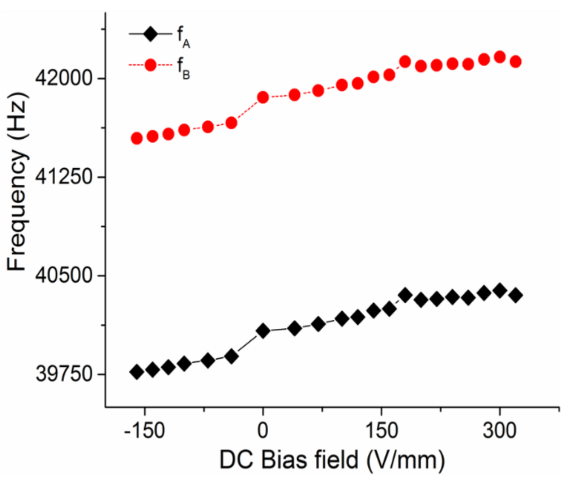

(a)

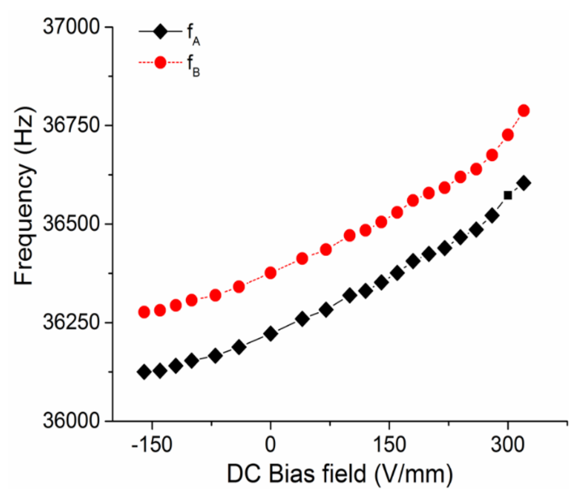

(b)

Figure 5.2.2 Type A and Type B resonance frequency change for (a) Hard PZT (b) Soft PZT

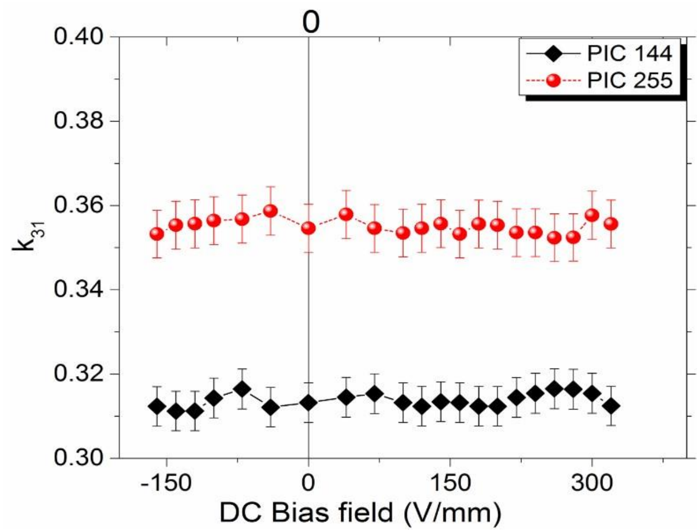

Figure 5.2.3 Electromechanical Coupling factor variation with the applied DC Bias field

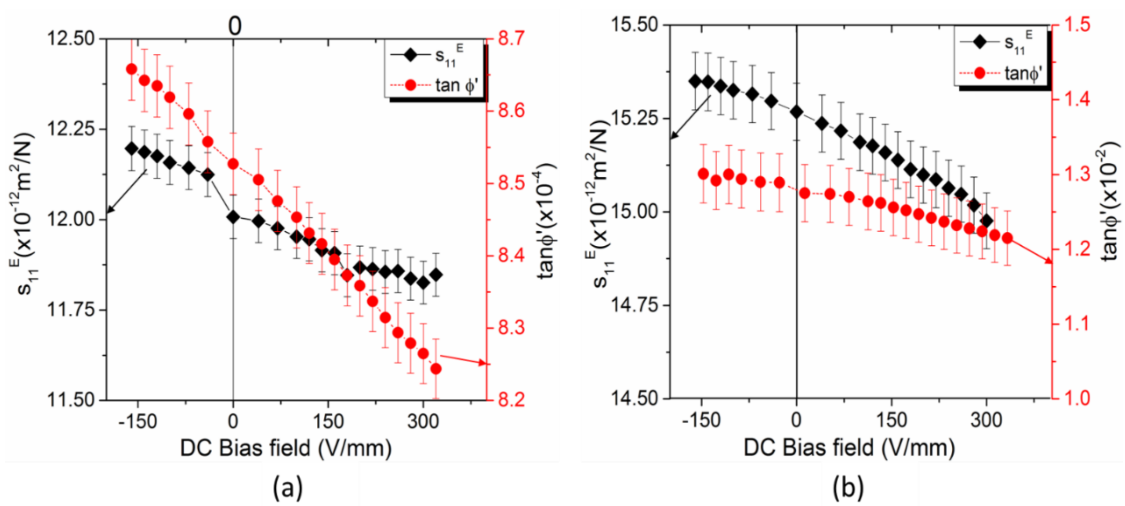

Figure 5.2.4 Elastic compliance and the corresponding loss for (a) Hard PZT (b) Soft PZT.

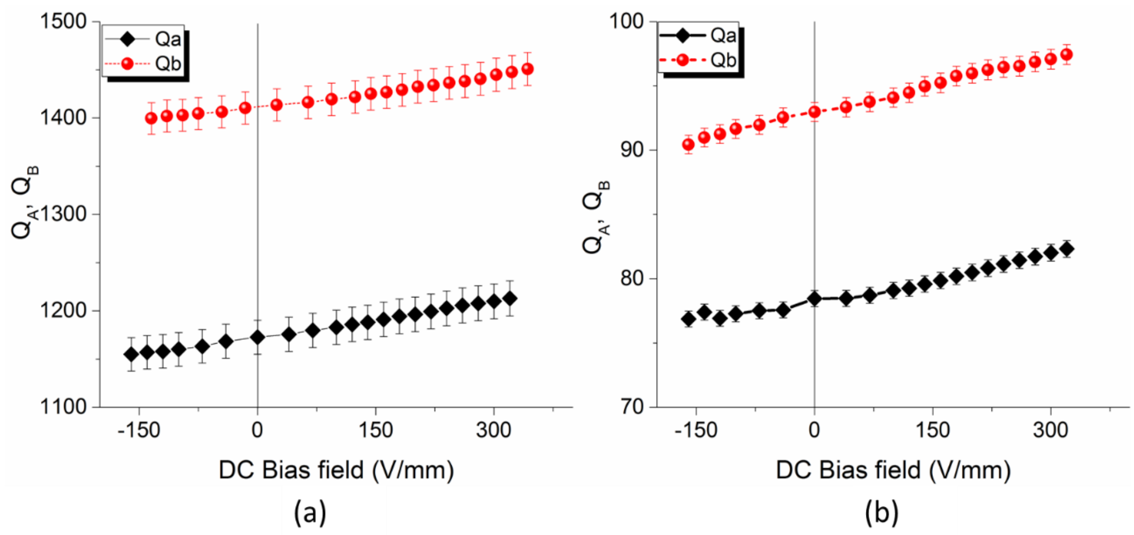

Figure 5.2.5 Quality factor variation at f_A and f_B with applied DC bias field for (a) Hard PZT (b) Soft PZT

5.2.3 Piezoelectric Constant and Piezoelectric Loss

In addition to the quality factor Q_A at the resonance condition, mechanical quality factor Q_B was also measured at the anti-resonance condition under DC bias field and plotted in Fig. 5.2.5. Thus, the piezoelectric constant and loss were determined from Eq. (5) as a function of the DC bias field (Fig. 5.2.6). The piezoelectric constant decrease for the hard PZT (- 1% per 100 V/mm) was less than for the soft PZT (- 1.5% per 100 V/mm) under a positive DC bias field. Also, apart from the real parameter, piezoelectric loss change of the hard PZT was again smaller (- 1.9% per 100 V/mm) for the hard PZT as compared to the soft PZT (- 3.1%). For negative DC bias field, the piezoelectric constant increase for the hard PZT (0.7% per 100 V/mm) was less than for the soft PZT (1.2% per 100 V/mm). Apart from that, piezoelectric loss change of the hard PZT was again smaller (1.5% per 100 V/mm) for the hard PZT as compared to the soft PZT (2.8% per 100V/mm). Also, it has been shown here that piezoelectric complex decreases with positive DC bias field which is just exactly opposite to the effect of negative DC Bias field.

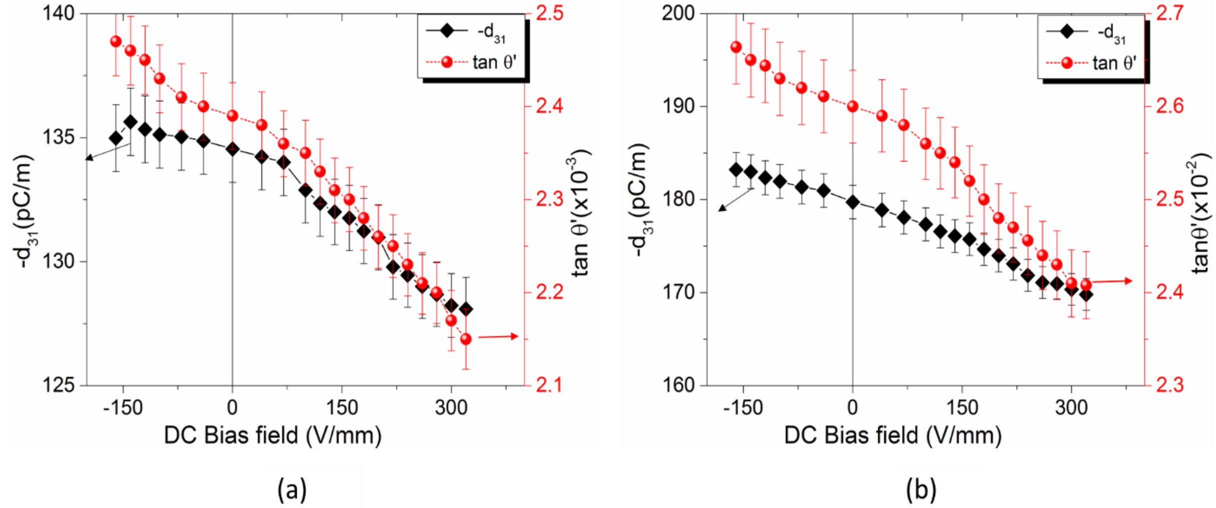

Figure 5.2.6 Variation of Piezoelectric complex with applied DC bias field for (a) Hard PZT (b) Soft PZT

5.3 High Power Measurements under DC Bias Field

High power measurements were conducted under externally applied DC bias field using the burst mode. Because the open-circuit burst drive was not available (external DC bias effect cannot be measured), only the short-circuit (under a constant E_{bias}) burst drive could be achieved. The elastic compliance, as well as the elastic loss for both samples were measured as a function of vibration velocities at various levels of externally applied DC bias field. Figures 5.3.1 and 5.3.2 shows respective two graphs demonstrating the variation of the elastic properties and the elastic loss tan φ' for the hard and soft PZT's. Positive DC bias field provided a decrease in both elastic compliance and loss. The % elastic loss decrease per 100 V/mm was noted to be - 2.5% for the hard PZT, whereas - 3.0% for the soft PZT under 30 mm/sec, which significantly increased - 3.5% for the hard and - 4.2% for the soft under 300 mm/sec. More precisely, the decrease rate is enhanced as the vibration velocity is increased for both the hard and soft PZT's. The elastic compliance increased with the rate of 2.9% for the hard PZT and 4.8% per 100 mm/sec for the soft PZT at a small DC bias field of 50 V/mm., while, as the DC bias field was increased to 300 V/mm, the % decrease in elastic compliance per 100 mm/sec was - 0.7% for the hard PZT and - 1.7% for the soft PZT. The % elastic loss decrease per 100 V/mm was noted to be - 2.5% for the hard PZT whereas - 3.0% for the soft PZT under 30 mm/sec, which are significantly enhanced to - 3.5% for the hard and - 4.2% for the soft under 300 mm/sec.

Likewise, it turns out to be essential to consider that negative DC bias field gives very nearly an equivalent and inverse change in the change of properties. It means that both elastic compliance and loss decreases with positive DC bias field which is just exactly opposite to the effect of negative DC Bias field. In conclusion, the external DC bias field affects more drastically to stabilize the high-power vibration excitation in the case of a positive bias field and destabilizes in the case of a negative bias field. Regarding the antiresonance measurement for determining the piezoelectric and dielectric losses, we will report an alternative way in successive papers.

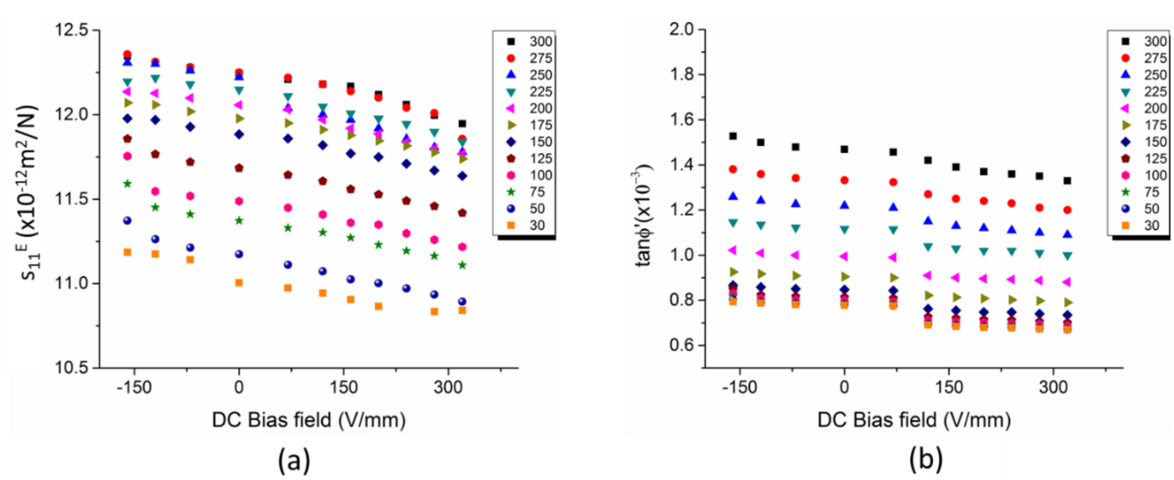

Figure 5.3.1 High power properties for hard PZT (a) Elastic compliances (b) Elastic loss

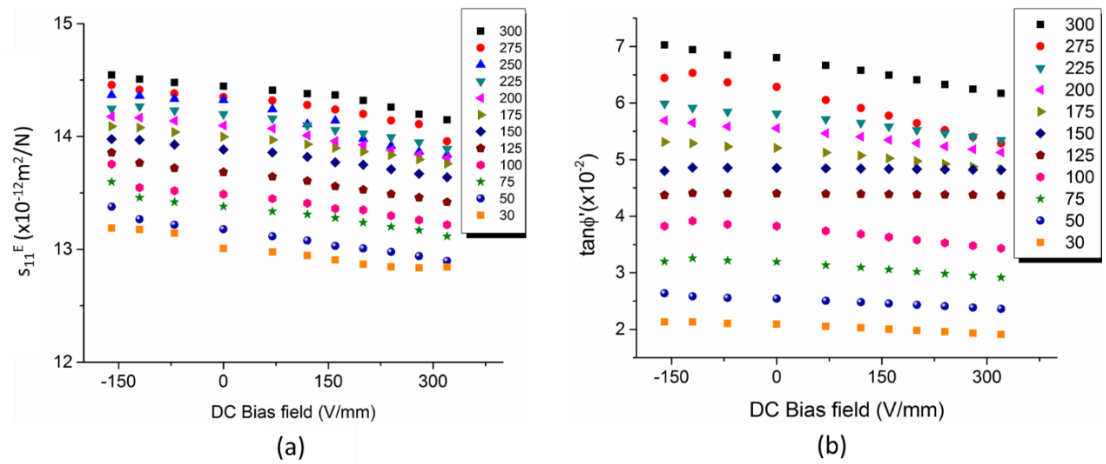

Figure 5.3.2 High power properties for soft PZT (a) Elastic compliance (b) Elastic lo

Chapter 6

Discussions and Summary

In this thesis, the dependency of dielectric, elastic and piezoelectric coefficients (real parameters and imaginary losses) on the vibration velocity and DC bias field comprehensibly was studied. Note that as the piezoelectric ceramic is driven at a high vibration velocity, introducing AC stress is intoduced in the material. Table 1 summarizes the material's coefficients change with the vibration velocity and DC electric field. Note that these results are not associated with any temperature rise during the measurements. It has been found that with the vibration velocity increase, the dielectric constant, elastic compliance, piezoelectric coefficient, and their corresponding losses increase for both the hard and soft PZT's. However, the change is more pronounced in the soft PZT as compared to the hard PZT. To the contrary the influence of a DC bias field depends strongly of the direction of the field with respect to the original poling field. A positive DC bias electric field affects in a way, that is, decrease in the dielectric constant, elastic compliance, piezoelectric coefficient and their corresponding losses, whereas a negative DC bias field affects in an completely opposite way. The decrease rate of these physical parameters under small vibration level is enhanced under large vibration level, as shown in the third column in Table 1. This situation can be visualized in the 3D plot in Fig. 18, showing the dependence of elastic loss tan φ' on the externally applied DC bias field and the vibration velocity at the k_{31} sample length edge in the hard (PIC 144) and soft (PIC 255) PZT. In comparison with a relatively smooth plane contour for the soft PZT, a clear bend on the contour plane is observed for the hard PZT. We can find the intensive elastic loss tan φ' shows two different trends under vibration velocity and DC bias field; increase with the vibration velocity (domain wall destabilization) and decrease with positive DC bias field (domain wall stabilization). Roughly speaking, the vibration velocity 100 mm/s (+3% and

5% change in s_{11}^E for the hard and soft PZT's) exhibits the almost equivalent "opposite" change rate (–1.7% × 2 and –2.3% × 2 change in s_{11}^E for the hard and soft PZT's) of 200 V/m DC electric field.

This equivalency can be understood roughly as follows. Like the off-resonance analysis in Ref. 20, the external stress X_1 is roughly estimated with the external electric field E_3 by

$$X_1 = (d_{31}/s_{11}^E)E_3 \qquad (6.1)$$

Conversely, the electric field induced by the stress is estimated by

$$E_3 = (d_{31}/\varepsilon_0\varepsilon_{33}^X)X_1. \qquad (\text{or } X_1 = (\varepsilon_0\varepsilon_{33}^X/d_{31})E_3) \qquad (6.2)$$

Since the electromechanical coupling factor $\frac{d_{31}}{\sqrt{\varepsilon_0\varepsilon_{33}^X s_{11}^E}}$ is not equal to 1, $d_{31}/s_{11}^E \neq \varepsilon_0\varepsilon_{33}^X/d_{31}$. Thus, we adopt a geometric average relationship for evaluating the equivalency:

$$X_1 = -\sqrt{\frac{\varepsilon_0\varepsilon_{33}^X}{s_{11}^E}}\, E_3 \qquad (6.3)$$

The sign "–" stands for the opposite effect owing to the transversal piezoelectric effect (i.e., $d_{31} < 0$). We may extend this relationship at the resonance by multiplying the mechanical quality factor Q_m:

$$|X_1| = Q_m\sqrt{\frac{\varepsilon_0\varepsilon_{33}^X}{s_{11}^E}}\, |E_3| \qquad (6.5)$$

Using practical values for the hard PZT (s_{11}^E = 12 x 10^{-12}, ε_{33}^X = 1100 and Q_m = 1200) and E_3 = 200 V/m, X_1 becomes 6.8 x 10^6 N/m^2. On the other hand, the relation between the maximum $X_{1,rms}$ (at the k_{31} plate sample center) and vibration velocity $v_{1,rms}$ (at the sample edge) is given by[19]

$$X_{1,rms} = \sqrt{\frac{\rho}{s_{11}^E}}\, v_{1,rms} \qquad (6.6)$$

Using practical values for the hard PZT (ρ = 7.5 x 10^3 and s_{11}^E = 12 x 10^{-12}) again, $v_{1,rms}$ = 100 mm/s provides $X_{1,rms}$ = 2.5 x 10^6 N/m^2 or $X_{1,peak}$ = 4.0 x 10^6 N/m^2, which shows a reasonable agreement (in the same order) with the value estimated by Eq. (6.4).

Another noteworthy point is the two-step mechanisms observed in the hard PZT: a bend of the slope can be observed in the elastic loss tan φ' on the vibration velocity change, while a bend of the slope in the dielectric constant ε_{33}^{X} and dielectric loss tan δ' is observed on the DC bias field change. This may suggest a sort of threshold value in terms of mechanical stress or electrical field in the hard PZT for stabilizing/destabilizing the domain wall motions. This may suggest a sort of domain stabilization threshold, and the detailed analysis of the results will be reported in successive papers.

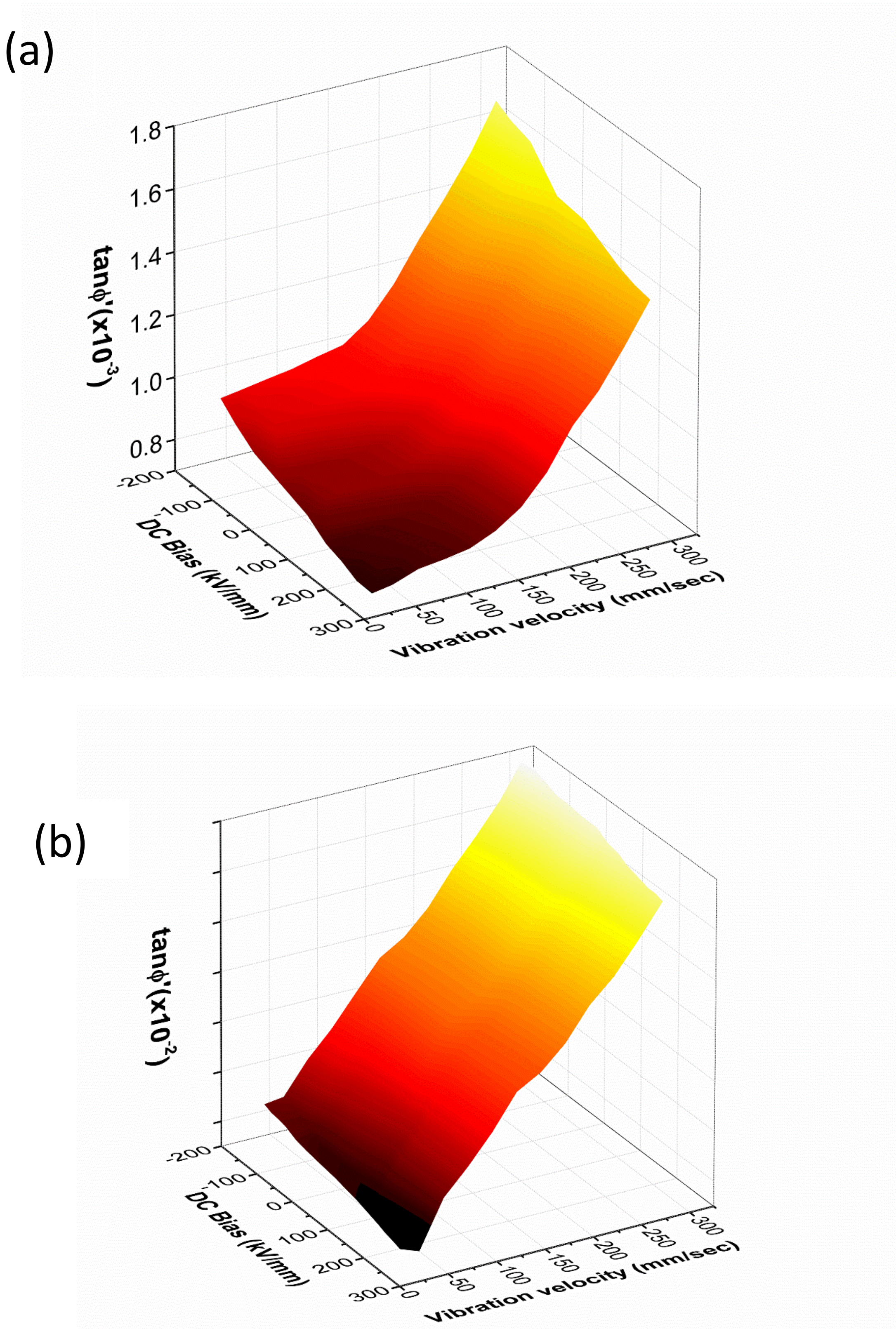

Figure 6.1 3D plot showing the variation of elastic loss for PZT's as a function of DC Bias field and vibration velocity for (a) Hard PZT (b) Soft PZT

Table 2 Table showing the change in material properties with applied positive DC bias field and vibration

% Change in material properties	Vibration velocity (per 0.1m/sec)		Electric field (per 100V/mm at 0.01m/s)		Electric field (per 100V/mm at 0.3m/s)	
	Hard PZT	Soft PZT	Hard PZT	Soft PZT	Hard PZT	Soft PZT
Dielectric Constant (ε_{33}^{T})	+2.9%	+5%	-0.8%	-1.7%	-	-
$\tan\delta'_{33}$	-	-	-0.4%	-1.5%	-	-
Elastic compliance (s_{11}^{E})	+3%	+5%	-0.7%	-1.7%	-1.7%	-2.3%
$\tan\varphi'_{11}$	+75%	(+)~0% & 75%	-1.1%	-2.4%	-3.5%	-4.2%
Piezoelectric constant (d_{31})	+2.7%	+5.1%	-1%	-1.5%	-	-
$\tan\theta'_{31}$	+70%	+20%	-1.9%	-3.1%	-	-
Electromechanical Coupling factor (k_{31})	+3.5%	+5.3%	Change within error limits	Change within error limits	-	-

Chapter 7
Future Research Topics

Piezoelectric ceramics such as Lead-Zirconia Titanates [$Pb(Zr_xTi_{1-x})O_3$, PZT's] have continued to dominate the market for a very long time now owing to its excellent properties and enormous application such as ultrasonic transducers, actuators, sensors etc. However, properties and performance of the device depends on the application it is being used in. Therefore, there is a critical need to measure the properties of the piezoelectric ceramic under different external electrical and mechanical boundary conditions. This thesis showed the effect of externally applied DC bias field (one of electrical boundary conditions) on the properties. Apart from this boundary condition, there is another major boundary condition which needs immediate analysis. Langevin transducer, one of the most used transducer, works under externally applied stress. This external boundary conditions must largely change the performance of the device. There is still less understanding on the effect of mechanical boundary conditions on the properties of piezoelectric ceramics and could be one of the future works to do.

The effect of the temperature on the high power performance can also be investigated by using the burst mode at different temperatures. These possible advances would create a better understanding of high power characteristics of the piezoelectric materials. Therefore, extra modifications can be done in the existing piezoelectric material systems to enhance high power characteristics.

Domain wall study of the piezoelectric ceramics under different externally applied electrical or mechanical boundary conditions is also another interesting area to be worked to understand the physical phenomenon of the loss behavior.

Bibliography

[1] Lu, Chao, and Alvin Warren Czanderna, eds. Applications of piezoelectric quartz crystal microbalances. Vol. 7. Elsevier, 2012.

[2] Munn, R. W. "Thermodynamic and physical properties of solids in electric fields." Journal of Physics C: Solid State Physics 6.22 (1973): 3213.

[3] Rodel, W. Jo, K. T. Seifert, E. M. Anton, and T. Granzow: J. Am. Ceram. Soc. 92 (2009) yang1153.

[4] C. Kittel: *Introduction to Solid State Physics* (John Wiley & Sons, Inc., Hoboken, 2005) 8th ed.

[5] K. Uchino, *Ferroelectric Devices* (CRC Presss, 2000)

[6] K. Uchino, J. Zheng, Y. H. Chen, X. Du, S. Hirose, and S. Takahashi: *IEEE Trans. UFFC 48* (2001).

[7] P. Home, T. Teaching, and C. Woodford, “Piezoelectricity,” pp. 1–7, 2016.

[8] D. Wang, J. S. Chen, "Progress on the Applications of Piezoelectric Materials in Sensors", Materials Science Forum, Vol. 848, pp. 749-756, 2016.

[9] H.N. Shekhani, K. Uchino, “Characterization of Mechanical Loss in Piezoelectric Materials Using Temperature & Vibration Measurements,” J. of American Ceramic Society, vol. 97, pp. 2810–2814, 2014.

[10] T. Ikeda: *Fundamentals of Piezoelectricity* (Oxford University Press, 1990).

[11] “Dielectric, elastic and Piezoelectric losses in Piezoelectric Materials; Gordon E. Martin Naval Undersea Center San Diego, California, 92132,” 1954.

[12] A. M. Bolkisev, V. L. Karlash, and N. A. Shul, “Temperature Dependence of the properties of piezoelectric ceramics,” Soviet Applied Mechanics 20.7 (1984): 650-653.

[13] D. Damjanovic, “Materials for high temperature piezoelectric transducers,” *Curr. Opin. Solid State Mater. Sci.*, vol. 3, no. 5, pp. 469–473, 1998.

[14] K. Uchino, "Materials issues in design and performance of piezoelectric actuators: an overview," *Acta Mater.*, vol. 46, no. 11, pp. 3745–3753, 1998.

[15] H. N. Shekhani and K. Uchino, "Evaluation of the mechanical quality factor under high power conditions in piezoelectric ceramics from electrical power," *J. Eur. Ceram. Soc.*, vol. 35, no. 2, pp. 541–544, 2015.

[16] H. N. Shekhani, E. A. Gurdal, S. O. Ural, and K. Uchino, "Analysis of High Power Behavior in Piezoelectric Ceramics from a Mechanical Energy Density Perspective," ArXiv ID: 1605.06685.

[17] B. Li, G. Li, S. Zhao, L. Zhang, and A. Ding, "Characterization of the high-power piezoelectric properties of PMnN–PZT ceramics using constant voltage and pulse drive methods," *J. Phys. D. Appl. Phys.*, vol. 38, no. 13, pp. 2265–2270, 2005.

[18] B. Fu, T. Li, and Y. Xie, "Model-based diagnosis for pre-stress of langevin transducers," *2009 IEEE Circuits Syst. Int. Conf. Test. Diagnosis, ICTD'09*, pp. 1–4, 2009.

[19] K. Adachi *et al.*, "Development of Bolt-Clamped Langevin-Type Transducer Factor for Excitation of Large Torsional Vibration with High Mechanical Quality." Jpn. J. Appl. Phys., vol. 33, no. 2, pp. 1182-1188, 1994.

[20] Y. Gao, K. Uchino, and D. Viehland, "Time dependence of the mechanical quality factor in 'hard' lead zirconate titanate ceramics: development of an internal dipolar field and high power origin," *Japanese J. Appl. Physics,* vol. 45, no. 12, pp. 9119–9124, 2006.

[21] A. J. Masys, W. Ren, G. Yang, and B. K. Mukherjee, "Piezoelectric strain in lead zirconate titante ceramics as a function of electric field, frequency, and dc bias," *J. Appl. Phys.*, vol. 94, no. 2, pp. 1155–1162, 2003.

[22] Yang, G., et al. "Effects of uniaxial stress and DC bias field on the piezoelectric, dielectric, and elastic properties of piezoelectric ceramics." Ultrasonics Symposium, 2000 IEEE. Vol. 2. IEEE, 2000.

[23] Wang, Qing-Ming, et al. "Effect of DC bias field on the complex materials coefficients of piezoelectric resonators." Sensors and Actuators A: Physical 109.1 (2003).

[24] S. Priya, S. O. Ural, H. W. Kim, K. Uchino, and T. Ezaki: *Jpn. J. Appl. Phys. 43* (2004)

[25] S. Priya, H. Kim, and K. Uchino: *Design Consideration for Nonlead Piezoelectric Transformers* The Pennsylvania State University (MRI, International Center for Actuators and Transducers, University Park, 2003).

[26] K. Ishii, N. Akimoto, S. Tashirio, and H. Igarashi: *J. Eur. Ceram. Soc. 19 (*1999).

[27] S.Hirose, Y. Yamayoshi, M. Taga, and H. Shimizu: *Jpn. J. Appl. Phys. 30* (1991).

[28] S. Takahashi, Y. Sasaki, S. Hirose, and K. Uchino: *Jpn. J. Appl. Phys. 34* (1995).

[29] H. Iwasaki, and T. Ikeda: J. Phys. Soc. Jpn. 18 (1963).

[30] Majzoubi, Maryam, et al. "Advanced methodology for measuring the extensive elastic compliance and mechanical loss directly in k31 mode piezoelectric ceramic plates." *J. of Appl. Phys* 120.22 (2016).

[31] H. Shekhani, T. Scholehwar, E. Hennig, and K. Uchino, “High Power Characterization of Piezoelectric Ceramics Using the Burst/Transient Method with Resonance and Antiresonance Analysis,” *J. Am. Ceram. Soc.*, Vol 10., pp. 1–21 (2016).